UNIVERSIDADE FEDERAL DE SANTA MARIA
CENTRO DE TECNOLOGIA
PROGRAMA DE PÓS–GRADUAÇÃO EM ENGENHARIA QUÍMICA

Gabriel Vanni

APROVEITAMENTO DE RESÍDUOS DO PROCESSAMENTO DE UVA PARA A BIOSSORÇÃO DE CORANTES E PRATA

Santa Maria, RS
2017

Gabriel Vanni

APROVEITAMENTO DE RESÍDUOS DO PROCESSAMENTO DE UVA PARA A BIOSSORÇÃO DE CORANTES E PRATA

Dissertação apresentada ao Curso de Mestrado do Programa de Pós–Graduação em Engenharia Química, da Universidade Federal de Santa Maria (UFSM, RS), como requisito parcial para obtenção do grau de **Mestre em Engenharia Química**.

Orientador: Prof. Dr. Guilherme Luiz Dotto

Co–orientadora: Prof. Dr. Leticia Belén Escudero

Santa Maria, RS

2017

Gabriel Vanni

APROVEITAMENTO DE RESÍDUOS DO PROCESSAMENTO DE UVA PARA A BIOSSORÇÃO DE CORANTES E PRATA

Dissertação apresentada ao Curso de Mestrado do Programa de Pós–Graduação em Engenharia Química, da Universidade Federal de Santa Maria (UFSM, RS), como requisito parcial para obtenção do grau de **Mestre em Engenharia Química**.

Aprovado em 5 de dezembro de 2017

Prof. Guilherme Luiz Dotto, Dr. (UFSM)
(Presidente/Orientador)

Prof. Tito Roberto Sant'Anna Cadaval Jr., Dr. (FURG)

Prof. Edson Luiz Foletto, Dr. (UFSM)

Santa Maria, RS
2017

AGRADECIMENTOS

Gostaria de agradecer meus pais Marcos Fernando Vanni e Juliandra Alves da Silveira Vanni pelo suporte que me deram ao longo de toda jornada acadêmica, foram muitas conversas e conselhos para eu seguir em frente e continuar buscando conhecimento.

Agradecer meu orientador, e chefe Guilherme Luiz Dotto, que se tornou uma pessoa essencial na minha formação de Mestre, pela oportunidade por ele dada a mim e a grande parceria que fizemos.

Também quero agradecer minha co-orientadora Leticia Belén Escudero pela oportunidade de trabalhar juntos e a parceria durante todos experimentos realizados em conjunto para a conclusão desse trabalho.

Quero agradecer aos Professores Edson Luiz Foletto e Tito Roberto Sant'Anna Cadaval Jr por serem banca e avaliarem meu trabalho.

Ao demais professores e funcionários do PPGEQ e todos aqueles que me ajudaram a formar opinião e sanar dúvidas durante todo o período que estive cursando o mestrado.

RESUMO

Neste trabalho foi investigado o potencial de resíduos da indústria de vinho como alternativa para remover os corantes Azul Brilhante (AB) e Vermelho Amaranto (VA) como também íons de prata em meio aquoso; todos experimentos foram realizados em batelada. Os resíduos foram triturados e peneirados até as partículas ficarem na faixa de 80 a 110 µm e nomeados de casca de uva, semente de uva, e engaço de uva. Estes materiais foram caracterizados de acordo com o ponto de carga zero (pH_{ZPC}), titulação de Boehm, espectroscopia de infravermelho de transformada de Fourier (FTIR), microscopia eletrônica de varredura (MEV), espectroscopia de energia dispersiva de raio-x (EDS) e mapeamento de raio-x. Nos experimentos com a semente de uva e corantes, a biossorção foi favorecida em pH 1 usando dosagem de 0.500 g L^{-1}, alcançando a remoção de 85%. Os modelos cinéticos de pseudo – segunda ordem e Elovich foram capazes de representar a cinética, e o equilíbrio foi representado pelos modelos de Langmuir e Sips. As máximas capacidades de biossorção foram de 599.5 e 94.2 mg g^{-1} para o AB e VA respectivamente, com processo espontâneo, favorável e endotérmico. Nos experimentos com os três biossorventes e íons de prata, a biossorção foi favorecida em pH 7 e dosagem de biossorvente de 3.0 g L^{-1}. A cinética foi bem representada pelo modelo de pseudo–primeira ordem e o equilíbrio pelo modelo de Sips. As máximas capacidades de biossorção encontradas em temperatura de 298 K foram: 41.7, 61.4, e 46.4 mg g^{-1} para casca, semente, e engaço respectivamente. A operação foi espontânea, favorável, exotérmica e controlada pela entalpia, configurando sorção física. Estes resultados demonstraram que os resíduos da indústria de vinho podem ser considerados uma alternativa eficiente de biossorventes de baixo custo, e ambientalmente ecológicos para remoção dos corantes AB e VA como também de íons de prata em meio aquoso.

Palavras–chave: Biossorventes, Resíduos de vinho, Corantes, Íons prata.

ABSTRACT

In this work, the potential of wine industry wastes as alternative biosorbents to remove Brilliant Blue (BB) and Amaranth Red (AR) dyes as also Ag ions from aqueous media was investigated; all experiments were performed in batch systems. The wastes were pulverized and sieved until the discrete particles size ranging from 80 to 110 μm and named grape peel (GPE), grape seeds (GSE), and grape stem (GST). These materials were characterized according to the point of zero charge (pH_{ZPC}), Boehm titration, Fourier transform infrared spectroscopy (FTIR), scanning electron microscopy (SEM), energy X–ray dispersive spectroscopy (EDS), and X–ray mapping. In experiments with GSE and dyes, the biosorption was favored at pH 1.0 using biosorbent dosage of 0.500 g L^{-1}, reaching 85% of removal percentage. The pseudo–second order and Elovich models were able to represent the kinetic data, and the Langmuir and Sips models represented the equilibrium. The maximum biosorption capacities were 599.5 and 94.2 mg g^{-1} for BB and AR, respectively, with spontaneous, favorable and endothermic process. In the experiments with the three biosorbents and silver ions, the biosorption was favored at pH 7.0 using biosorbent dosage of 3.0 g L^{-1}. The kinetic data were well represented by the pseudo–first order model and the equilibrium by the Sips model. The maximum biosorption capacities, found at 298 K, were: 41.7, 61.4, and 46.4 mg g^{-1} for GPE, GSE, and GST, respectively. The process was spontaneous, favorable, exothermic, and enthalpy–controlled, configuring physical sorption. These results showed that the wine industry wastes can be considered alternative efficient, low–cost, and eco–friendly biosorbents to remove the BB and AR dyes as also Ag ions from aqueous media.

Keywords: Biosorbents, Wine wastes, Dyes, Silver ions.

LISTA DE FIGURAS

LISTA DE TABELAS

SUMÁRIO

1 INTRODUÇÃO

Em décadas recentes a atividade industrial cresceu, aumentando o uso de água em todo o mundo, liberando vários poluentes para o meio ambiente, como metais pesados, corantes, entre outros (ABDOLALI et al., 2014). Indústrias que utilizam corantes em seus processos constituem um dos maiores problemas de tratamento de efluentes devido à alta demanda química e biológica de oxigênio, sólidos suspensos e componentes tóxicos (aromáticos, metais, cloretos). Estes efluentes diminuem significantemente a atividade fotoquímica da vida aquática, devido ao impedimento da penetração da luz (AKSU, 2005). A contaminação por metais pesados tornou–se um problema global devido à sua toxicidade elevada, maior bioacumulação na cadeia alimentar e natureza não–biodegradável, além de serem cancerígenos aos seres humanos (HE; CHEN, 2014).

Muitas técnicas de remediação para remover íons metálicos vêm sendo empregadas, desde processos físico–químicos (precipitação química, osmose reversa, oxidação/redução, tratamento eletroquímico e filtração) a métodos de bioremediação (bioacumulação, biossorção e fitoremediação) (VIJAYARAGHAVAN; BALASUBRAMANIAN, 2015). Para efluentes contendo corantes são usados processos que combinam a floculação com flotação, eletrofloculação, filtração por membrana, destruição eletroquímica, precipitação, resina de troca iônica, biossorção, entre outros (SRINIVASAN; VIRARAGHAVAN, 2010). Entretanto, estas técnicas não são efetivas para remoção economicamente viável de metais pesados e corantes com concentrações de 500mg L^{-1} ou menos, desta forma o uso da biossorção ganhou atenção por se tratar de uma operação simples e viável, onde o uso de carvão ativado na operação alcança a remoção de 99% de íons metálicos. O carvão ativado é o biossorvente mais usado, também possibilitando tratar efluentes contendo corantes (ABDOLALI et al., 2014; DOTTO et al., 2015; FAROOQ et al., 2010).

Na busca por materiais de baixo custo, a biossorção vem emergindo como uma tecnologia alternativa ambientalmente amigável para remoção de corantes e íons metálicos com algumas vantagens (biossorvente de baixo custo, processo rápido, fácil operação do processo, alta remoção de contaminantes e insensibilidade a substâncias tóxicas) (DOTTO; LIMA; PINTO, 2012; FAROOQ et al., 2010). Assim vários materiais veem sendo investigados para serem usados como biossorventes de baixo custo como materiais naturais (madeira, turfa, carvão, quitina, etc) e resíduos ou

subprodutos industrial/agrícola (argilas, cinzas, bagaço) (GUPTA; SUHAS, 2009). Nesse contexto, resíduos da uva tem grande potencial para serem usados como biossorventes (FARINELLA; MATOS; ARRUDA, 2007). A produção de vinhos e suco de uva no Brasil está concentrada no Rio Grande do Sul com produção média anual de 300 milhões de litros. Os resíduos (bagaço e sementes) da uva usada para vitificação equivalem a aproximadamente 20% em peso da uva e os resíduos usados para elaboração de sucos de uva equivalem a 25% em peso de uva (MELLO; SILVA, 2014). Com base nestas informações, este trabalho busca usar os resíduos da uva que são o engaço, casca e semente para reaproveitamento como biossorventes na operação de biossorção, visando a diminuição da quantidade de prata e corantes em soluções sintéticas.

2 OBJETIVOS

2.1 OBJETIVOS GERAIS

Este trabalho teve como objetivo geral verificar o desempenho de resíduos do processamento de uva (engaço, casca e semente) como biossorventes na operação de biossorção de íons de prata e corantes (azul brilhante e vermelho amaranto).

2.2 OBJETIVOS ESPECÍFICOS

- Obter e caracterizar os resíduos (engaço, casca e semente) do processamento de uva;
- Estudar o efeito da massa e do pH na biossorção da prata e corantes (azul brilhante e vermelho amaranto) pelos resíduos do processamento da uva;
- Estudar a cinética de biossorção;
- Estudar o equilíbrio de biossorção;
- Estudar a termodinâmica de biossorção;
- Verificar interações físico–químicas dos biossorventes com a prata e corantes;
- Simular efluentes e tratar nas melhores condições.

3 REVISÃO BIBLIOGRÁFICA

3.1 PROBLEMATICAS DOS EFLUENTES

Com o crescimento da humanidade, sociedade, ciência, tecnologia nosso mundo está caminhando para novos horizontes, mas o custo disso já está tendo consequências de desordem ambiental como um grande problema de poluição (GUPTA; SUHAS, 2009). Segundo a UNESCO, o uso de água pela agricultura, indústria e setores domésticos tem aumentado muito, cerca de 70, 22 e 8% respectivamente (THE UNITED NATIONS, 2003). Alguns poluentes como metais pesados ou compostos orgânicos clorados contaminam fontes aquáticas e afetam a cadeia alimentar podendo se acumular no organismo animal, afetando principalmente o topo da cadeia alimentar. Os principais poluentes da água incluem uma variedade de químicos orgânicos (corantes), inorgânicos (metais pesados) e compostos industriais, afetando a saúde humana e interferindo no uso industrial ou na agricultura (CES Technical Report 113)

É relatado que existem cerca de 100,000 corantes disponíveis comercialmente com a produção de cerca de $7x10^5$ toneladas por ano (AKSU, 2005). As moléculas de corantes compreendem dois componentes principais: os cromóforos, responsáveis pela cor e os auxocromos que produzem cor e tornam a molécula solúvel em água, produzindo maior afinidade com fibras (HUNGER; WILEY–VCH, 2003). Muitas indústrias, especialmente de alimentos e têxtil, frequentemente usam corantes e pigmentos em seus produtos, perdendo 10–20% dos corantes durante a fabricação, e consequentemente, produzindo uma grande quantidade de efluentes coloridos (DOTTO; LIMA; PINTO, 2012). Não menos importante é a contaminação por metais pesados, que podem vir a serem lançados para o meio ambiente em processos naturais ou atividades antropogênicas, mais comumente por indústrias de galvanoplastia, fundição de metais e indústrias químicas (CHOWDHURY et al., 2016).

Corantes são usados em vários ramos da indústria incluindo borracha, têxtil, cosméticos, plástico, couro, alimentos e papel. Uma variabilidade de corantes é vista nos efluentes descarregados pelas indústrias. Geralmente corantes são estáveis à luz, calor e agentes oxidantes, normalmente tem origem sintética e estrutura molecular aromática complexa, o que torna mais estável e difícil sua biodegradação (KONO, 2015). O principal problema no tratamento de efluentes contendo corantes e seus metabólitos é que alguns podem ser mutagênicos e cancerígenos além de também serem xenobióticos na natureza e recalcitrantes (GUPTA et al., 2013).

Corantes podem ser classificados de acordo com seus derivados, podem ser de origem natural ou sintética. Corantes naturais são extraídos de fontes incluindo plantas, animais e minerais, estes corantes foram usados largamente durante o início da indústria têxtil (DAWOOD; SEN, 2014). Corantes sintéticos têm substituído corantes naturais e incluem corantes básicos, ácidos, reativos, diretos, vat e dispersos (CHEN et al., 2011).

Os cromóforos em corantes aniônicos e catiônicos são na maioria grupos azo ou compostos do tipo antraquinona; a redução da clivagem nas ligações azo é responsável pela formação de aminas tóxicas nos efluentes. Os corantes baseados em antraquinona são mais resistentes a degradação devido às suas estruturas aromáticas fundidas e assim fornecem cor por um longo período de tempo nos efluentes (AKSU, 2005).

Corantes reativos são tipicamente cromóforos azo combinados com diferentes tipos de grupos reativos (vinilsulfona, clorotriazina, tricloropiridina, difluorocloropirinida), sendo diferentes de todas as outras classes de corantes na sua ligação com fibras têxteis como algodão através de ligações covalentes, conferindo características de cor brilhante e rápida diluição, porém corantes reativos e ácidos são os mais problemáticos, uma vez que, tendem a passar pelo sistema convencional de tratamento sem efetividade de remoção (ROBINSON et al., 2001).

Corantes básicos têm alto brilho e intensidade de cor (são altamente visíveis em pequenas concentrações), já corantes com complexos metálicos são na maioria baseados em cromo (elemento cancerígeno) (PRASAD; SINGH, 1990)(BANAT et al., 1997). Quando se trata de corantes dispersivos, há a tendência de bioacumulação, uma vez que não ionizam em meio aquoso (BANAT et al., 1997).

Tem sido reportado que metais pesados afetam as organelas celulares e componentes, e algumas enzimas envolvidas no metabolismo, intoxicam e provocam danos irreparáveis, além disso, eles têm bioacumulação natural em sistemas bióticos e provocam danos a seres humanos e animais mesmo em concentrações pequenas (STAWINSKI et al., 2017). Considerando o impacto ao meio ambiente por metais, os três mais problemáticos são o mercúrio, chumbo e cádmio. O menos problemático destes é o mercúrio que vem sendo substituído por novas tecnologias na indústria; já o chumbo que tinha como principal fonte a gasolina, como fonte de contaminação bem definida, vem sendo fornecida sem chumbo. Enquanto o mercúrio e o chumbo são limitados e não estão em uma tendência de aumentar o seu consumo, cádmio é tóxico e seu uso vem aumentando estando presente em muitos processos por todo o mundo

apresentando potencial perigo aos seres humanos e ao meio ambiente (HOLANT, 1995).

3.2 MÉTODOS DE TRATAMENTO

Efluentes contendo corantes sintéticos ou metais pesados podem causar danos potencialmente perigosos ao meio ambiente. Devido ao impacto ambiental e às preocupações de saúde associadas a estes efluentes, uma série de técnicas tem sido usada para remover corantes ou metais pesados de soluções aquosas, em que podem ser divididos em físicos, químicos e biológicos. Cada método de separação tem suas próprias limitações em termos de design, eficiência de remoção e custo total (DAWOOD; SEN, 2014).

Devido ao alto custo e problemas de disposição final, muitas dessas técnicas de tratamento não têm sido aplicadas em larga escala (CES Technical Report 113). Na Tabela 1 estão apresentadas as técnicas e suas respectivas vantagens e desvantagens (DAWOOD; SEN, 2014; YAGUB et al., 2014):

A biossorção tem sido usada para remoção de cor e tem boa aplicabilidade em tratamento de efluentes (GUPTA; SUHAS, 2009). O termo biossorção refere–se a acumulação de substâncias na interface entre duas fases (sólido–líquido ou sólido–gás) (DABROWSKI, 2001). Resinas de troca iônica (membranas sólidas, folha sólida, solução de solvente orgânico) são materiais sólidos ou soluções líquidas que são capazes de absorver íons carregados positivamente ou negativamente de soluções aquosas eletrólitas e ao mesmo tempo descarregam outros íons na mesma quantidade para a solução aquosa (DAWOOD; SEN, 2014).

A tecnologia de filtração inclui a microfiltração, ultrafiltração, nanofiltração e osmose reversa. Dentre a filtração as técnicas mais efetivas para remoção de corantes são a ultrafiltração e nanofiltração, pelo seu tamanho de poro, são usadas em tratamento de efluentes têxtis, porém seus pontos fracos são a alta pressão de trabalho, alto consumo de energia, e alto custo da membrana que tem pequeno tempo de uso (CHEREMISINOFF, 2002).

Tabela 1 – Técnicas de remoção de corantes e metais.

Técnicas	Vantagens	Desvantagens
Tratamentos físicos		
Biossorção	Alta capacidade de biossorção para diferentes corantes	Baixo custo
Resina de troca iônica	Sem perda de biossorventes	Não é efetivo para corantes dispersos
Filtração por membrana	Remoção de todos os tipos de corantes	Produção de lodo. Para baixos volumes
Coagulação eletrocinética	Economicamente praticável	Alta produção de lodo
Tratamentos químicos		
Reação Fenton	Aplicado conforme a característica química	Geração de lodo
Destruição eletroquímica	Sem consumo de agentes químicos e de formação de lodo	Altas vazões causam a à redução na remoção dos corantes
Fotoquímico	Redução dos odores e sem geração de lodo	Formação de produtos indesejáveis
Processos oxidativos	Simplicidade de aplicação	Agente precisa de ativação
Tratamentos biológicos		
Descolorização por fungos	Alguns fungos são capazes de decompor corantes utilizando enzimas	Já foi demonstrado quer a produção de enzimas é inviável.
Mistura de culturas microbianas	Tempo de descolorização de 24 a 30 horas	Sob condições aeróbias os azo corantes não estão prontos para serem metabolizados
Uso de biomassa de microrganismos	Afinidade relativa ao tipo de corante e microrganismos	Não é efetivo para todos os tipos de corantes
Sistema de bioremediação anaeróbica têxtil–corante	Permite a descolorização de azo corantes e corantes solúveis em água	A quebra anaeróbica gera metano e sulfito hidrogenado

Adaptado de: DAWOOD; SEN, 2014, p. 1–11, Yagub et al, 2014, p. 175.

Na coagulação eletrocinética é usado um metal (aluminio ou ferro) como eletrodo imersso no efluente para causar dissolução desse metal, formando íons que coagulam para flocular partículas formando hidróxidos que precipitam e quimicamente adsorvem contaminantes químicos (CHEN, 2004). É um processo simples que se comparado com técnicas concencionais como coagulação química não gera poluição secundária, além de ser um equipamento compacto (DAWOOD; SEN, 2014).

A efetividade dos métodos químicos depende da interação entre os contaminantes presentes no efluente e a natureza do produto químico usado, podendo ter a função de separar ou modificar e neutralisar os efeitos nocivos ao meio ambiente. Estas técnicas são boas para descolorir a água porém ao mesmo tempo são de alto custo e inferiores porque produzem uma grande quantidade de lodo, e portanto há um problema de descarte de lodo (NGULUBE et al., 2017).

Os processos oxidativos são tradicionalmente usado para remover subtâncias inorgânicas e orgânicas de efluentes. Oxidantes químicos são muito efetivos mas sua eficácia é fortemente influenciada pelo tipo de oxidante que pode incluir cloreto, ozônio, Fenton e dióxido de cloro (DAWOOD; SEN, 2014)

3.3 BIOSSORÇÃO

Biossorção é um processo de sorção, onde uma biomassa é usada como biossorvente. O fenômeno da biossorção foi observado no início dos anos 1970 quando elementos radioativos (incluindo metais pesados) nos efluentes liberados de uma estação de força nuclear foram encontrados concentrados em algas (HE; CHEN, 2014). Os principais pontos fortes da biossorção são a alta seletividade e eficiência, baixo custo de operação, altas taxas de remoção e uso de materiais naturais que são abundantes (AKSU, 2005).

O mecanismo de remoção de metais geralmente inclui biossorção física, troca iônica, quelação, complexação e micro–precipitação (VEGLIO; BEOLCHINI, 1997). A biossorção envolve uma variedade de mecanismos independentes no processo que tem como responsável essencialmente a parede celular da biomassa, devido a altas forças atrativas capazes de captar diferentes metais de acordo com o tipo de biomassa usada, que incluem algas, fungos, bactérias, resíduos industriais, resíduos da agricultura e

outros materiais a base de polissacarídeos (VIJAYARAGHAVAN; BALASUBRAMANIAN, 2015). Foram encontrados uma variedade de grupos funcionais presentes na parede celular que oferecem certas forças de atração (para compostos, íons metálicos, etc.) e promovem o aumento da eficiência de remoção (FAROOQ et al., 2010).

Ao se tratar de remoção de corantes, recentemente uma série de estudos focaram nas biomassas que são capazes de biodegradar ou biossorver corantes de efluentes, como turfa, quitosana, leveduras, fungos e biomassa bacteriana (SRINIVASAN; VIRARAGHAVAN, 2010). As variações de corantes e sua química resultam em diversas interações entre o corante e o biossorvente (CRINI, 2006). A biossorção de corantes é dependente das propriedades do corante como estrutura molecular e tipo, número e posição dos substituintes das moléculas do corante (REIFE; FREEMAN, 1996).

3.4 ESTUDOS UTILIZANDO BIOSSORVENTES PARA REMOÇÃO DE METAIS E CORANTES

Na procura por alternativas para substituir o carvão ativado por biossorventes sustentáveis, pesquisadores veem usando materiais diversos encontrados em estado natural ou resíduos industriais que podem vir a serem modificados para melhorar sua eficiência. Visto que existem inúmeros trabalhos publicados a respeito do uso de biossorventes para remoção de corantes e metais, serão comentados alguns casos estudados para remoção especificamente dos corantes Azul Brilhante e Vermelho Amaranto como também estudos para remoção de íons de prata.

Dotto e Pinto (2011) realizaram o estudo de biossorção do corante Azul Brilhante com quitosana a partir de resíduos de camarão. Os autores otimizaram as condições do processo com pH 3, agitação de 150 rpm e tempo de 60 minutos em temperatura de 25°C obtendo capacidade de biossorção de 210 mg g^{-1} com o uso do modelo cinético Elovich.

Rajeshkannan et al. (2011) conduziram o estudo da remoção do corante Azul Brilhante a partir de biomassa marinha. A biomassa usada foi a *Hydrilla Verticillata* e as condições ótimas do processo foram: concentração inicial de corante em meio aquoso de 100 mg L^{-1}, temperatura de 30°C, pH 3, quantidade de biossorvente 2.88 g L^{-1} com tamanho de partícula de 0.124 mm, tempo de contato de 180 min e velocidade de

agitação de 237 rpm. Com essas condições foi possível obter a capacidade de biossorção de 38.46 mg g^{-1}.

Ho e Chiang (2001) estudaram a sorção do corante Azul Brilhante (Acid Blue 9) com uma mistura de argila ativada e carvão ativado. O estudo revelou que a isoterma de Langmuir é a que melhor se ajusta ao processo com condições ótimas de pH 3, temperatura de 30°C foi possível a obtenção da capacidade de biossorção de 53.6 mg g^{-1}.

Cadaval Jr. et al. (2015) fizeram o estudo da remoção do corante Vermelho Amaranto (Acid Red 27) com filmes de quitosana. O melhor modelo para representar o equilíbrio da reação foi o de Langmuir. Neste estudo foram usados os seguintes parâmetros: pH 2, concentração inicial de corante na solução de 100 mg L^{-1} e temperatura de 25°C alcançando a capacidade de biossorção de 494.13 mg g^{-1} com um processo de biossorção exotérmico, espontâneo e favorável.

Guerrero–Coronilla et al. (2015) realizaram o estudo da biossorção do corante Vermelho Amaranto por folhas de Jacinto aquáticas. Neste estudo os autores notaram que a biossorção aumentava com o aumento do tempo de contato e com a concentração inicial do corante e, também com a diminuição do tamanho de partículas das folhas e pH da solução. As condições ótimas para o processo foram pH 2, temperatura de 25°C alcançando a capacidade de biossorção de 70 mg g^{-1} e revelando que o processo foi endotérmico e não espontâneo.

Ahalya et al. (2013) conduziram o estudo de biossorção do corante Vermelho Amaranto usando como biossorvente cascas de tamarindo. O melhor modelo que se ajustou para a cinética do processo foi o de pseudo primeira ordem sob pH 2 alcançando a capacidade de biossorção de 65 mg g^{-1}. A partir da técnica de análise FTIR foi possível constatar os seguintes grupos funcionais sob a superfície do biossorvente: –OH, –COOH, C=O e C–O.

Jeon (2015) estudou o comportamento da biossorção de íons de prata em solução usando um biossorvente feito de cascas de caranguejo em pó. O biossorvente foi imobilizado em forma de pérola por um método de aprisionamento utilizando álcool polivinílico e ácido bórico, obtendo diâmetro de 2 mm e área superficial de 11.124 m^2 g^{-1} estável até 45°C e pH 10. O pesquisador obteve remoção de 83% de íons de prata da solução com 4 g de biossorvente e capacidade de biossorção de 2.951 mg g^{-1} de prata em pH 6.

Cantuaria et al (2015) realizaram o estudo da biossorção de íons de prata em meio aquoso usando sistema batelada com um biossorvente de argila bentonita termicamente modificado. A partir de um modelo de transferência de massa os pesquisadores concluíram que o processo era principalmente controlado por transporte externo e o melhor modelo de equilíbrio foi o de Langmuir. A máxima capacidade e biossorção para o biossorvente foi de 61.48 mg g^{-1} em 283 K e 55.55 mg g^{-1} em 293 K, além disso a tendência de aumento da capacidade de biossorção para temperaturas mais elevadas indica que o processo é exotérmico; esses fatos foram verificados pelos parâmetros termodinâmicos o que conclui que o processo é espontâneo e governado por biossorção física.

Beigzadeh e Moeinpour (2016) estudaram o comportamento do biossorvente de cinzas de aloe vera suportado em nanopartículas de $Ni0.5Zn0.5Fe_2O_4$. Os pesquisadores fizeram testes em diferentes pH (2–7), doses de biossorvente (0.01–0.5 g) e obtiveram um alto valor de remoção (98%) e a máxima capacidade de biossorção de 243.9 mg g^{-1} para o íon de prata nas condições de 30 min de contato e pH 5, além disso o biossorvente produzido possui grande área superficial (814.23 m^2 g^{-1}) e volume de poros (0.726 cm^3 g^{-1}).

Em geral, os estudos acima mencionados mostram a importância da busca de novos matérias, cada vez com menor custo, melhores características e maior eficiência, para a remoção de contaminantes de meios aquosos por biossorção.

3.5 ISOTERMAS DE BIOSSORÇÃO

Modelos de equilíbrio têm sido extensivamente usados para investigar a quantidade de íons de metálicos ou corantes adsorvidos por diversos biossorventes (FAROOQ et al., 2010). Estes modelos de equilíbrio são denominados de isotermas e tem grande importância para explicar como ocorre a interação do biossorvente com o adsorbato, fornecendo também a capacidade máxima de biossorção (YAGUB et al., 2014).

A distribuição dos íons de determinada substância entre a solução e o biossorvente pode ser calculada por estas isotermas, onde a fase na superfície do biossorvente pode ser considerada como monocamada ou multicamada dependendo do modelo usado para explicar o processo (YAGUB et al., 2014). Os modelos mais usados em estudos aplicados a biossorção são o modelo de Langmuir e o modelo de Freundlich,

também podem vir a serem usados os modelos de Langmuir–Freundlich, Redlich–Peterson, Brunaur–Emmer–Teller (BET) e Sips (AKSU, 2005; LIU; LIU, 2008).

De acordo com o modelo de Langmuir (1918), a sorção ocorre na superfície do biossorvente de maneira homogênea e os átomos/íons formam uma monocamada, com sítios energeticamente iguais, na superfície do biossorvente. Apesar de não dar informações sobre o mecanismo, ele ainda é usado para mensurar a capacidade de biossorventes, conforme a equação 1 (Langmuir, 1918):

$$q_e = \frac{q_m K_L C_e}{1 + K_L C_e} \tag{1}$$

onde, q_e é a capacidade de biossorção no equilíbrio (mg g^{-1}), C_e é a concentração do adsorbato no equilíbrio (mg L^{-1}), q_m é a capacidade máxima de biossorção (mg g^{-1}) e K_L é a constante de Langmuir (L mg^{-1}). Outro importante aspecto no modelo de Langmuir é o fator de equilíbrio, R_L, conforme a equação (2):

$$R_L = \frac{1}{1 + K_L C_e} \tag{2}$$

Para R_L = 1, a isoterma é linear, 0< R_L <1 indica que o processo é favorável e, R_L =0 indica que o processo é irreversível (HAMDAOUI; NAFFRECHOUX, 2007).

Ao contrário da isoterma de Langmuir, Freundlich (1906) descreve as características de biossorção com camada heterogênea na superfície do biossorvente (NGULUBE et al., 2017), conforme a equação matemática (3):

$$q_e = K_f C_e^{\frac{1}{Nf}} \tag{3}$$

onde, q_e é a capacidade de biossorção no equilíbrio (mg g^{-1}), C_e é a concentração do adsorbato no equilíbrio (mg L^{-1}), *1/Nf* é o fator de heterogeneidade e K_F é a constante de Freundlich (mg g^{-1})(mg L^{-1})$^{-1/nF}$.

Outro modelo de isoterma foi proposto por Sips (1948), também nomeado de Langmuir–Freundlich é essencialmente a isoterma de Freundlich que se aproxima da máxima biossorção em altas concentrações de adsorbato. Este modelo pode ser obtido assumindo que a biossorção acontece em monocamada na superfície, mas que a biossorção é um processo cooperativo devido a interações biossorvente–adsorbato (AKSU, 2005). A isoterma de Sips está na equação (4):

$$q_e = \frac{q_s (K_s C_e)^m}{1 + (K_s C_e)^m} \quad (4)$$

onde, q_s é a capacidade máxima de biossorção (mg g^{-1}), K_s é a constante de Sips (mg L^{-1}) e m é o expoente de Sips.

Similar à isoterma de Sips, Redlich–Peterson propôs uma isoterma que possui as características de Langmuir e de Freundlich, apresentada na equação geral que segue (5):

$$q_e = \frac{K_{rp} C_e}{1 + a_{rp} C_e^{\beta}} \quad (5)$$

sendo, K_{rp} (L g^{-1}) e a_{rp} (L mg^{-1}) de são constantes de Redlich–Peterson e β é o expoente do modelo. A equação (5) reduz à isoterma de Langmuir quando o exponente é igual a um e resulta na equação da lei de Henry se β for igual a zero (CES Technical Report 113).

3.6 TERMODINÂMICA DE BIOSSORÇÃO

Através da isoterma de biossorção é possível calcular os parâmetros termodinâmicos da biossorção (ΔS^{o}, ΔH°, ΔG°). Estes parâmetros servem para indicar a espontaneidade da biossorção, o tipo de biossorção e o mecanismo do processo, bem como a influência da temperatura na biossorção. Geralmente, a determinação dos parâmetros termodinâmicos é realizada pela equação de Van`t Hoff (6) (GHOSAL; GUPTA, 2016):

$$ln(\rho K_e) = \frac{\Delta S^{\circ}}{R} - \frac{\Delta H^{\circ}}{RT} \quad (6)$$

onde ΔG° é a variação da energia livre de Gibbs padrão (kJ mol^{-1}), ΔH° é a variação da entalpia padrão (kJ mol^{-1}), $\Delta S°$ é a variação da entropia padrão (kJ mol^{-1} K^{-1}), K_e é a constante de equilíbrio (L g^{-1}) e ρ é massa especifica da solução (g L^{-1}).

O parâmetro ΔG° pode ser obtido pelas equações (7) e (8):

$$\Delta G^0 = -RT\ln\left(\rho K_e\right) \quad (7)$$

$$\Delta G^0 = \Delta H^0 - T\Delta S^0 \quad (8)$$

Valores positivos e negativos de ΔH° representam reação endotérmica e exotérmica, respectivamente. Valores positivos de ΔS° refletem a afinidade do biossorvente com o adsorbato; o aumento da aleatoriedade na interface sólido–líquido aumenta o grau de liberdade do adsorbato e condições mais favoráveis para ocorrência do processo de biossorção. No entanto, valores de $\Delta S°$ negativos implicam na redução da biossorção. Valores negativos de $\Delta G°$ refletem em um processo de biossorção espontânea, já valores positivos implicam em processo não espontâneo (GHOSAL; GUPTA, 2016).

3.7 CINÉTICA DA BIOSSORÇÃO

Com o passar dos anos uma grande variedade de modelos cinéticos (pseudo primeira ordem, pseudo segunda ordem, ordem geral, Elovich, Crank, Boyd, Bangham, Weber e Morris, etc) de biossorção foram formulados.

Há três etapas em um processo de biossorção, em primeiro lugar há a transferência de massa da solução para a superfície externa do biossorvente, seguindo–se de difusão interna do adsorbato para os sítios de sorção e finalmente a própria sorção. Alguns modelos são baseados no fato de a sorção ser o passo limitante da velocidade na biossorção, outros supõem que a difusão é o passo limitante da taxa, assim a adaptação aos modelos permite a elucidação do mecanismo de biossorção (LARGITTE; PASQUIER, 2016).

Os modelos cinéticos de pseudo–primeira ordem e pseudo–segunda ordem são baseados na capacidade de biossorção. O modelo de pseudo–primeira ordem (equação 9) é geralmente aplicável após os primeiros 20–30 min do processo de sorção, enquanto o modelo de pseudo segunda ordem (equação 10) é adequado para todo o intervalo de tempo de contato (DOTTO; COSTA; PINTO, 2013).

A equação cinética de pseudo–primeira ordem ou também chamada de equação de Lagergren é dada por (HE; CHEN, 2014):

$$q_t = q_1(1 - \exp(-k_1 t)) \tag{9}$$

onde q_t é a quantidade de adsorbato adsorvido no tempo t (mg g $^{-1}$), q_1 é o valor teórico da capacidade de biossorção (mg g^{-1}), k_1 é a constante de pseudo primeira ordem (min $^{-1}$) e t é o tempo (min).

A equação cinética de pseudo–segunda ordem é dada por (HE; CHEN, 2014):

$$q_t = \frac{t}{\left({}^{1}/_{k_2 q_2^2}\right) + ({}^{t}/_{q_2})} \tag{10}$$

onde q_t é a quantidade de adsorbato adsorvido no tempo t (mg g^{-1}), q_2 é o valor teórico da capacidade de biossorção (mg g^{-1}), k_2 é a constante de pseudo–segunda ordem (min $^{-1}$) e t é o tempo (min).

A equação cinética de Elovich primeiramente foi proposta por Roginsky e Zeldovich em 1934, e agora é conhecida geralmente como equação de Elovich, tem sido extensivamente aplicada a dados de biossorção, e é expressada pela equação (11) (LIU; LIU, 2008):

$$q_t = \frac{1}{b}\ln(1 + abt) \tag{11}$$

onde q_t é a quantidade de adsorbato adsorvido no tempo t (mg g^{-1}), a é a velocidade inicial devido a dq/dt com $q_t = 0$ (mg g^{-1} min^{-1}), b é a constante de desorção de Elovich e t é o tempo (min).

3.8 RESÍDUOS DE UVA

A uva é fonte natural de compostos fenólicos e está relacionada com importantes benefícios a saúde, devido as suas propriedades anti–inflamatórias, anti–carcinogênicas e por sua proteção contra doenças cardiovasculares. No Brasil as variedades de uvas americanas *Vitis labrusca L.* são amplamente cultivadas, principalmente para a elaboração de sucos (FRANKEL et al., 1998).

Durante o processo de elaboração do suco de uva ocorre à geração do resíduo denominado bagaço e do resíduo da centrifugação do suco. O bagaço (cascas e semente) é obtido na etapa de prensagem, e é fonte de compostos fenólicos e antioxidantes, promovendo o interesse da indústria de alimentos em sua utilização como matéria prima. Estes resíduos obtidos no processamento da uva apresentam elevado teor de umidade, sendo que a secagem destes resíduos é uma alternativa para prolongar sua vida útil e reduzir possíveis alterações químicas (SANTANA, 2015). A estabilidade dos compostos fenólicos durante a secagem do alimento está relacionada com a temperatura utilizada e com o tempo de exposição ao calor (ERBAY; ICIER, 2009).

A viticultura no Brasil é desenvolvida tradicionalmente nas regiões Sul, Sudeste e Nordeste, sendo uma atividade consolidada e com grande importância socioeconômica. O estado do Rio Grande do Sul é responsável por cerca de 90% da produção nacional de vinhos, sucos e derivados do país. O Brasil em 2012 produziu 830,92 milhões de kg (57,07%) de uvas destinadas à elaboração de derivados, o restante da produção 624,89 milhões de kg (42,93%) foi destinada ao consumo in natura. A produção total de uvas no Brasil neste mesmo ano foi de 1.455.809 milhões de kg, sendo o estado do Rio Grande do Sul o maior produtor com 840.251 milhões de kg. A produção de suco de uva em 2012 apresentou aumento de 75,55% em relação ao ano anterior incluindo suco concentrado transformado em suco simples e em suco de uva integral (SANTANA, 2015).

A tabela 2 apresenta uma estimativa da quantidade de bagaço de uva disponibilizado no ano de 2011, categorizada pelos dois grandes grupos (americanas e híbridas), e pela cor da película (tinta, branca e rosada). O grande volume é de uvas tintas (81,37%), sendo que as americanas e híbridas são as de maior volume e representam 75,08% do total deste tipo de resíduo (MARIA; MELLO, 2014).

Tabela 2 – Disponibilidade de bagaço de uva por tipo, em kg – Rio Grande do Sul – 2011.

Descriminação	Americanas e Híbridas	Viníferas	Total	(%)
Tintas	106.569.139	8.938.090	115.507.228	81,37
Rosadas	3.060.564	69.878	3.130.442	2,21
Brancas	15.760.289	7.548.464	23.308.753	16,42
Todas	125.389.992	16.556.432	141.946.424	100.00

Fonte: MARIA, L.; MELLO, R. DE. Comunicado155 Técnico. p. 1–6, 2014.

Em 2011, as 50 maiores vinícolas geraram cerca de 130 mil toneladas de bagaço e sementes de uvas. Destaca–se que a maior empresa processadora de uvas foca sua atividade na produção de suco de uvas, e, portanto, utiliza cultivares americanas e híbridas, em especial, as tintas. Os resíduos dessa empresa são encaminhados para uma empresa de compostagem. Essa empresa gerou, em 2011, cerca de 37 milhões de quilos de resíduos, sendo 7 milhões de quilos de engaço e 30 milhões de bagaço (casca e sementes) (MARIA; MELLO, 2014). Os resíduos de uva obtidos da etapa de prensagem são denominados de bagaço e são constituídos de cascas e sementes, representando de 12 a 15 % do peso da matéria–prima inicial. Os resíduos obtidos da etapa de centrifugação do suco de uva são constituídos pelos sólidos suspensos do suco e representam aproximadamente 4 a 8 % do volume inicial (SANTANA, 2015).

A baga geralmente é constituída de 6 a 12% de casca, 2 a 5% de semente e 85 a 92% de polpa. A polpa é constituída majoritariamente por 65 a 85% de água, 12 a 25% de açúcares redutores, 0,6 a 1,4% de ácidos orgânicos, 0,25 a 0,5% de substâncias minerais, 0,05 a 0,1% de compostos nitrogenados e diversas vitaminas hidrossolúveis e lipossolúveis (SANTANA, 2005). As sementes das uvas são compostas aproximadamente por 40% de fibra, 16% de óleo, 11% de proteínas, 7% de compostos fenólicos complexos (taninos), açúcares, sais minerais, etc. Possuem grande quantidade de compostos fenólicos monoméricos, tais como (+)–catequina, (–)–epicatequina e (–)–epicatequina–3–O–galato, e diméricos, triméricos e tetraméricos procianidinas, estes atuam como agentes antimutagênicos e antivirais (JAYAPRAKASHA; SELVI; SAKARIAH, 2003).

4 RESULTADOS E DISCUSSÃO

Os resultados e discussão deste trabalho estão apresentados na forma de dois artigos, os quais estão publicados nas revistas *Water Science and Technology* de qualis B1 e *Chemical Engineering Communications* de qualis A1 na área de engenharias II.

- ARTIGO 1: POWDERED GRAPE SEEDS (PGS) AS AN ALTERNATIVE BIOSORBENT TO REMOVE PHARMACEUTICAL DYES FROM AQUEOUS SOLUTIONS. Gabriel Vanni, Leticia B. Escudero, Guilherme L. Dotto. Publicado na *Water Science and Technology. vol. 76 no. 5 1177-1187. doi: 10.2166/wst.2017.307.*

- ARTIGO 2: BIOSORPTION OF SILVER FROM AQUEOUS SOLUTIONS USING WINE INDUSTRY WASTES. Leticia B. Escudero, Gabriel Vanni, Tássia Segger, Fábio A. Duarte, Guilherme L. Dotto. Publicado na *Chemical Engineering Communications. Accepted author version posted online: 20 Oct 2017. https://doi.org/10.1080/00986445.2017.1387856.*

ANEXO 1

4.1 ARTIGO 1: POWDERED GRAPE SEEDS (PGS) AS AN ALTERNATIVE BIOSORBENT TO REMOVE PHARMACEUTICAL DYES FROM AQUEOUS SOLUTIONS

Gabriel Vanni[1], Leticia Belén Escudero[2,3], Guilherme Luiz Dotto[1]*

.

[1]Chemical Engineering Department, Federal University of Santa Maria, 97105–900, Santa Maria, Brazil

[2]Consejo Nacional de Investigaciones Científicas y Técnicas (CONICET), Argentina

[3]Laboratory of Analytical Chemistry for Research and Development (QUIANID), Facultad de Ciencias Exactas y Naturales, Universidad Nacional de Cuyo, Padre J. Contreras 1300, (5500) Mendoza, Argentina.

*Corresponding author: e–mail: guilherme_dotto@yahoo.com.br

ABSTRACT

An alternative, low–cost and efficient biosorbent, powdered grape seeds (PGS), was prepared from wastes of a wine industry, and used to remove Brilliant Blue (BB) and Amaranth Red (AR) dyes from aqueous solutions. The biosorbent was properly characterized before and after the biosorption operation. The potential of PGS to remove BB and AR dyes was investigated thought kinetic, isotherm and thermodynamic studies. The biosorption of BB and AR was favored at pH 1.0 using biosorbent dosage of 0.500 g L^{-1}, being attained more than 85% of removal percentage. For BB and AR dyes, pseudo–second order and Elovich models were able to explain the biosorption kinetic. The biosorption equilibrium of BB on PGS was well represented by the Langmuir model, while for AR, the Sips model was the most adequate. The maximum biosorption capacities were 599.5 and 94.2 mg g^{-1} for BB and AR, respectively. The biosorption of BB and AR on PGS was a spontaneous, favorable and endothermic process. These findings indicated that PGS is a low–cost and efficient biosorbent, which can be used to treat dye containing waters.

Keywords Biosorbent; grape seeds; kinetic; pharmaceutical dyes; thermodynamic

INTRODUCTION

Dyes are commonly employed in pharmaceutical formulations to enhance the aesthetic appearance and reduce errors in medication (Pérez–Ibarbia *et al.* 2016). During the pharmaceutical manufacturing, some of these dyes are lost, and consequently, discarded in effluents (Fernández *et al.* 2010). The incorrect disposal of dye–containing effluents is a well know problem, which can cause several damages to the environment and human health (Gupta & Suhas 2009). In this way, some countries created severe restrictions for the discharge of colored effluents (Hessel *et al.* 2007), and consequently, many studies have been focused to search treatments able to remove dyes from aqueous effluents (Crini & Badot 2008; Álvarez *et al.* 2013; Yagub *et al.* 2014; Dotto *et al.* 2015a; Khandare & Govindwar 2015).

Several treatments are used to remove dyes from industrial effluents, including, chemical precipitation, ion flotation, ion exchange, membrane filtration, AOP's, adsorption, biosorption and electrochemical methods (Yagub *et al.* 2014; Ahmed *et al.* 2017). Among these, biosorption, which is defined as, "the removal of contaminants from aqueous media by inactive or non–living biomass", has gained attention due advantages like low cost, ease of operation, fast kinetics and use of diverse types of biomasses as biosorbents (Dotto *et al.* 2015a). In this sense, several biosorbents have been used to remove dyes from aqueous media, for example, papaya seeds (Weber *et al.* 2014), lotus seedpod (He *et al.* 2016), spent bleaching earth (Belhaine *et al.* 2016) and oricuri fiber (Meili *et al.* 2017). The use of grape wastes has been studied in the last years. Torab–Mostaedi *et al.* (2013) verified the potential of grape peels to remove cadmium and nickel from aqueous media. Al Bsoul *et al.* (2014) studied the potential of grape seeds as biosorbent for cooper ions. In spite of these efforts, the use of grape seeds as biosorbent for dye removal is scarce.

Currently, there is a great interest in the exploitation of the residues generated by the wine industry (Spiridon *et al.* 2016; Al–Hamamre *et al.* 2017). During wine production, it is estimated that approximately 25% of the grape weight results in by–product/waste (termed ‘pomace’ which is comprised of skins and seeds) (Dwyer *et al.* 2014). Grape seeds contain oil, lignin, cellulose and hemicellulose (Yedro *et al.* 2015). These compounds in turn, contain several functional groups that can act as biosorption sites. Based on these information's, we believe that grape seeds can be an available, low

cost and efficient material, which can be used as biosorbent to remove dyes from aqueous media.

In this research, an alternative low–cost and efficient biosorbent named powdered grape seeds (PGS) was prepared from wastes of a wine industry, and used to treat synthetic solutions containing the pharmaceutical dyes Brilliant Blue (BB) and Amaranth Red (AR). The biosorbent was characterized according to the point of zero charge (pH_{zpc}), Boehm titration, Fourier transform infrared spectroscopy (FT–IR), scanning electron microscopy (SEM) and energy X–ray dispersive spectroscopy (EDS). The effects of initial pH of the solution and biosorbent dosage on the biosorption were studied. The biosorption kinetic data were evaluated by the pseudo–first order, pseudo–second order and Elovich models. Langmuir, Freundlich and Sips models were used to fit the biosorption equilibrium data. Thermodynamic parameters such as, standard Gibbs free energy change (ΔG^0), standard enthalpy change (ΔH^0) and standard entropy change (ΔS^0) were also estimated.

MATERIALS AND METHODS

Preparation of powdered grape seeds (PGS) biosorbent

Powdered grape seeds (PGS) biosorbent was prepared from wastes of a wine industry located in Mendoza, Argentina. *Vitis vinifera L.* grapes were collected from vineyards located in Mendoza province, Argentina (33º04´S, 68º19´W). The grapevine bunches (red cultivar of the *Bonarda* variety) were subjected to the wine processing. During the wine processing, a pomace containing husks, stems and seeds was generated. This pomace was refrigerated and carried to the laboratory. The grape seeds were manually separated from the pomace, washed with drinking water and then rinsed with Milli–Q water. The seeds were lyophilized for 48 h (Virtis freeze mobile, model 6, USA), pulverized with a mill (Ultracomb, MO–8100A, Argentina) and sieved until the discrete particle size ranging from 80 to 110 μm. The resulting material was named powdered grape seeds (PGS) biosorbent.

Characterization techniques

The PGS biosorbent was characterized according to several important aspects regarding biosorption. The point of zero charge (pH_{zpc}) was determined using the eleven points experiment (Park & Regalbuto 1995), in order to assess the surface charge of the biosorbent as a function of the pH. The total acidity and basicity of the biosorbent was verified by the Boehm titration method (Goertzen *et al.* 2010). Fourier transform infrared spectroscopy (FT–IR) (Shimadzu, Prestige 21, Japan) was used to identify the main functional groups of the biosorbent (Silverstein *et al.* 2007). The textural characteristics of the biosorbent and the main elements on the surface were vizualized by scanning electron microscopy (SEM) coupled to energy X–ray dispersive spectroscopy (EDS) (Jeol, JSM–6610LV, Japan) (Goldstein *et al.* 1992). FT–IR and SEM were also performed after the biosorption process (optimum condition) in order to verify possible modifications on the biosorbent surface.

Pharmaceutical dyes

Two dyes commonly found in pharmaceutical effluents were selected to perform the study: Brilliant Blue (BB) and Amaranth Red (AR), both with industrial grade and purity higher than 85%. Brilliant Blue (BB) (Triphenylmethane dye, molecular weight 792.8 g mol^{-1}; C.I. 42090; λ_{max} = 408 nm) and Amaranth Red (AR) (azo dye, molecular weight 604.5 g mol^{-1}; C.I. 16185; λ_{max} = 521 nm) were supplied by a local manufacturer (Duas Rodas Ind. Jaraguá do Sul, Brazil) and were used without further purification. The three dimensional structural formulae of the dyes are shown in Figure 1. The solutions were prepared with distilled water and the reagents were of analytical grade.

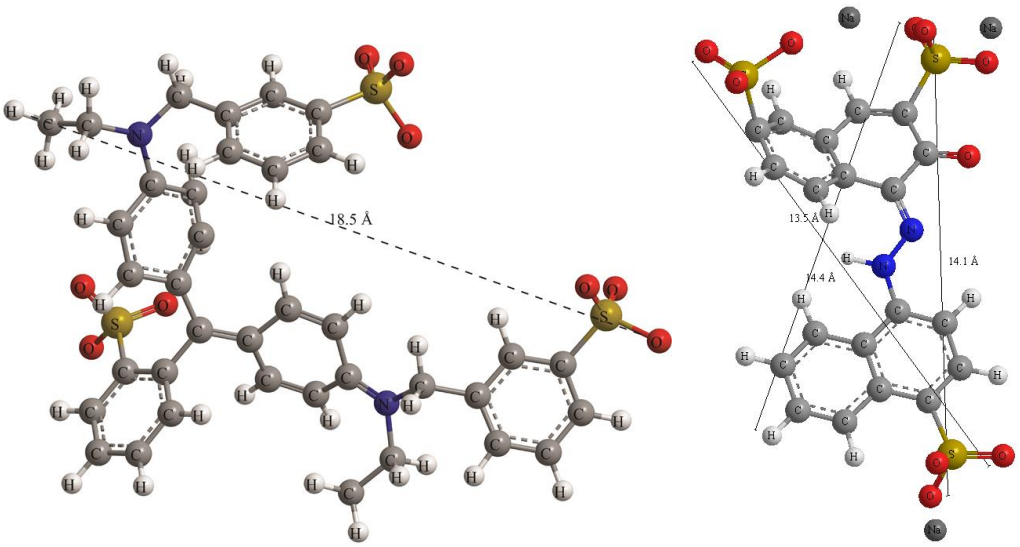

(a) (b)

Figure 1 Three dimensional structural formulae of the dyes: (a) Brilliant Blue (BB) and (b) Amaranth Red (AR).

Biosorption experiments

The biosorption experiments were realized in batch mode at 200 rpm using a thermostated agitator (Marconi, MA 093, Brazil) in order to verify the effects of initial pH, PGS dosage and also to obtain the kinetic and isotherm curves. Four experimental steps were performed:

- The effect of initial pH was studied (from 1.0 to 8.0) (adjusted with HNO_3 and NaOH) under the following conditions: initial dye concentration of 50 mg L^{-1}, contact time of 1 h, volume of solution of 25 mL, PGS dosage of 2.00 g L^{-1} and temperature of 25 °C (PGS was put directly in contact with the solutions);
- II) The effect of PGS dosage (from 0.25 to 5.00 g L^{-1}) was investigated under the same conditions, using the optimum pH defined elsewhere;
- III) Kinetic experiments were performed using the optimum pH and PGS dosage defined above. The initial dye concentration was 50 mg L^{-1}. The experiments were performed at 25 °C with contact time varying from 0 to 120 min and the volume of solution was 25 mL;
- IV) Isotherm curves were constructed at 25, 35, 45 and 55 °C, using the optimum pH and PGS dosage defined above. The initial dye concentration ranged from

25 to 300 mg L^{-1} and the volume of solution was 25 mL, being the aliquots stirred until the equilibrium (maximum 6 h).

After all the experiments, the solid phase was separated by centrifugation (Centribio, 80–2B, Brazil) at 4000 rpm for 20 min (Dotto *et al.* 2017) and, the remaining dyes concentration in the liquid phase was measured by spectrophotometry at the maximum wavelength for each dye (Biospectro SP–22, Brazil). To guarantee the experimental accuracy, the experiments were realized in replicate (n=3) using closed vessels and, blanks were performed. The dye removal percentage (*R*, %), mass of dye biosorbed per gram of biosorbent at any time (q_t (mg g^{-1})) and at equilibrium (q_e (mg g^{-1})) were calculated as follows (Crini & Badot 2008):

$$R = \frac{(C_0 - C_e)}{C_0} 100 \quad (1)$$

$$q_t = \frac{(C_0 - C_t)}{W} V \quad (2)$$

$$q_e = \frac{(C_0 - C_e)}{W} V \quad (3)$$

where, C_o, C_t, C_e (mg L^{-1}) are the dye concentrations at t=0, at any time and at equilibrium, respectively, W (g) is the biosorbent amount and V (L) is the volume of the solution.

Biosorption kinetics, isotherms and thermodynamics

The biosorption kinetics, isotherms and thermodynamics are fundamental investigations which should be performed in order to evaluate an alternative biosorbent material (Liu & Liu 2008). From the kinetic viewpoint, the biosorption of BB and AR pharmaceutical dyes on PGS was evaluated by the pseudo first–order (Lagergren 1898), pseudo second–order (Ho & Mckay 1998) and Elovich models (Zeldowitsch 1934), as follows:

$$q_t = q_1(1 - \exp(-k_1 t)) \quad (4)$$

$$q_t = \frac{t}{(1/k_2 q_2^2) + (t/q_2)} \quad (5)$$

$$q_t = \frac{1}{b} \ln(1 + abt) \quad (6)$$

where, k_1 and k_2 are the rate constants of pseudo first–order and pseudo second–order models, respectively in (min^{-1}) and (g mg^{-1} min^{-1}), q_1 and q_2 are the theoretical values

for the biosorption capacity (mg g^{-1}), a is the initial velocity due to dq/dt with q_t=0 (mg g^{-1} min^{-1}), b is the desorption constant of the Elovich model (g mg^{-1}) and, t is the time (min).

From the equilibrium viewpoint, the BB and AR biosorption on PGS was studied using the Langmuir (Langmuir, 1918), Freundlich (Freundlich 1906) and Sips (Sips 1948) isotherm models, as follows:

$$q_e = \frac{q_m K_L C_e}{1+(K_L C_e)} \quad (7)$$

$$q_e = K_F C_e^{1/n_F} \quad (8)$$

$$q_e = \frac{q_S (K_S C_e)^m}{1+(K_S C_e)^m} \quad (9)$$

being, q_m is the maximum biosorption capacity (mg g^{-1}), K_L is the Langmuir constant (L mg^{-1}), K_F is the Freundlich constant (mg g^{-1})(mg $L^{-1})^{-1/nF}$, $1/n_F$ is the heterogeneity factor, q_S the maximum biosorption capacity from Sips model (mg g^{-1}), K_S the Sips constant (L mg^{-1}) and m the Sips exponent. Another important aspect of the Langmuir model is the equilibrium factor, R_L:

$$R_L = \frac{1}{1+(K_L C_e)} \quad (10)$$

For R_L=1, the isotherm is linear, 0<R_L<1indicates a favorable process and, R_L=0 indicates an irreversible process (Hamdaoui & Naffrechoux 2007).

From the thermodynamic viewpoint, the biosorption of BB and AR was evaluated according to the standard values of Gibbs free energy change (ΔG^0, kJ mol^{-1}), enthalpy change (ΔH^0, kJ mol^{-1}) and entropy change (ΔS^0, kJ mol^{-1} K^{-1}), which were estimated by the combination of the following equations (Zhou *et al.* 2012; Anastopoulos & Kyzas 2016):

$$\Delta G^0 = -RT\ln(\rho K_e) \quad (11)$$

$$\Delta G^0 = \Delta H^0 - T\Delta S^0 \quad (12)$$

$$\ln(\rho K_e) = \frac{\Delta S^0}{R} - \frac{\Delta H^0}{RT} \quad (13)$$

where, K_e is the equilibrium constant (L g^{-1}) (based in the parameters of the best fit isotherm model), T is the temperature (K), R is 8.31x10^{-3} kJ mol^{-1} K^{-1} and is the solution density (g L^{-1}).

Parameters estimation

The kinetic and equilibrium parameters were estimated through nonlinear regression, minimizing the least squares function and using the Quasi–Newton estimation method. The Statistic 9.1 software (Statsoft, USA) was used to perform the calculations (El–Khaiary & Malash, 2011). The fit quality was measured through determination coefficient (R^2), adjusted determination coefficient (R^2_{adj}) and average relative error (*ARE*) (Dotto *et al.* 2013), as follows:

$$R^2 = \left(\frac{\sum_i^n \left(q_{i,exp} - \bar{q}_{i,exp}\right)^2 - \sum_i^n \left(q_{i,exp} - q_{i,model}\right)^2}{\sum_i^n \left(q_{i,exp} - \bar{q}_{i,exp}\right)^2} \right) \quad (14)$$

$$R^2_{adj} = 1 - \left(1 - R^2\right)\left(\frac{n-1}{n-p}\right) \quad (15)$$

$$ARE = \frac{100}{n}\sum_{i=1}^{n}\left|\frac{q_{i,\mathrm{model}} - q_{i,\mathrm{exp}}}{q_{i,\mathrm{exp}}}\right| \quad (16)$$

where, $q_{i,model}$ is each value of q predicted by the fitted model, $q_{i,exp}$ is each value of q measured experimentally, $\bar{q}_{i,\mathrm{exp}}$ is the average of q experimentally measured, n is the number of experimental points and p is the number of parameters.

RESULTS AND DISCUSSION

Characteristics of powdered grape seeds (PGS) biosorbent

PGS biosorbent was characterized according to the point of zero charge (pH_{zpc}), total acidity and basicity, FT–IR, SEM and EDS. The pH_{zpc} of the biosorbent was 6.85 (see supplementary material). This shows that at pH values lower than 6.85 the biosorbent is positively charged, while at pH values higher than 6.85, PGS is negatively charged. The values of carboxylic, lactonic and phenolic groups were, respectively, 0.05, 0.28 and 2.98 meq g^{-1}. Consequently, the total acidity on the PGS surface was 3.31 meq g^{-1}. The total basicity was 0.01 meq g^{-1}.

The FT–IR spectra of PGS biosorbent before (PGS) and after the biosorption process (PGS loaded BB and PGS loaded AR are depicted in Figure 2.

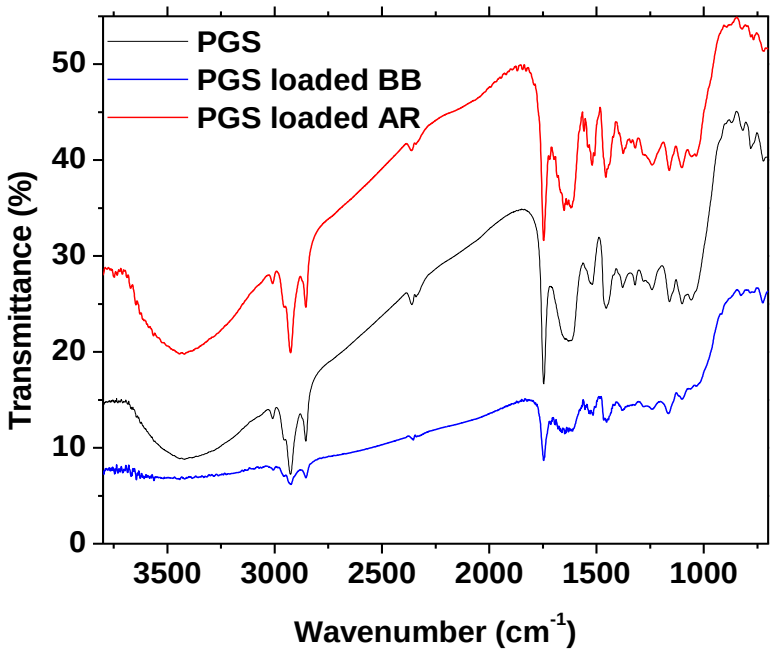

Figure 2 FT–IR spectra of PGS biosorbent before (PGS) and after the biosorption process (PGS loaded BB and PGS loaded AR).

The PGS spectrum (before biosorption) in Figure 2 shows the main intense bands around 3400, 2900, 2800, 1750, 1650, 1510, 1400 and from 1300 to 1000 cm^{-1}. The broad band centered at 3400 cm^{-1} is the –OH stretching. The stretchings of C–H and CH_2 can be vizualized at 2900 and 2800 cm^{-1}, respectively. The band at 1750 cm^{-1} could be assigned to the carbonyl groups (C=O). The C=O link of the acetyl groups can be seen at 1650 cm^{-1}. The C=C link of aromatic ring is vizualized at 1510 cm^{-1}. The CH deformation can be seen at 1400 cm^{-1}. The vibrational bands in the region 1300–1000 cm^{-1} can be assigned to –CO, C–O–C and carboxylic acids. These bands reveal that the PGS biosorbent is composed by several functional groups that are able to bind with the pharmaceutical dyes AR and BB. In the spectra after biosorption (PGS loaded BB and PGS loaded AR) (Figure 2), no significant changes were observed. This shows that no links were formed or broken during the biosorption process, indicating that a physical biosorption occurred.

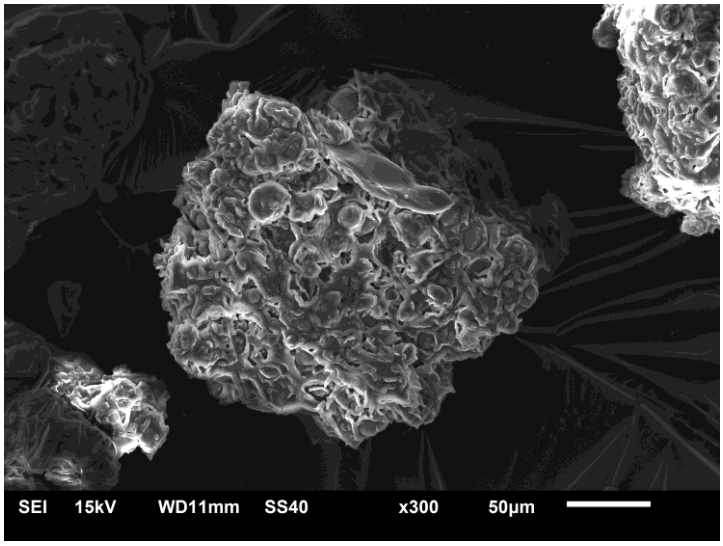

(a)

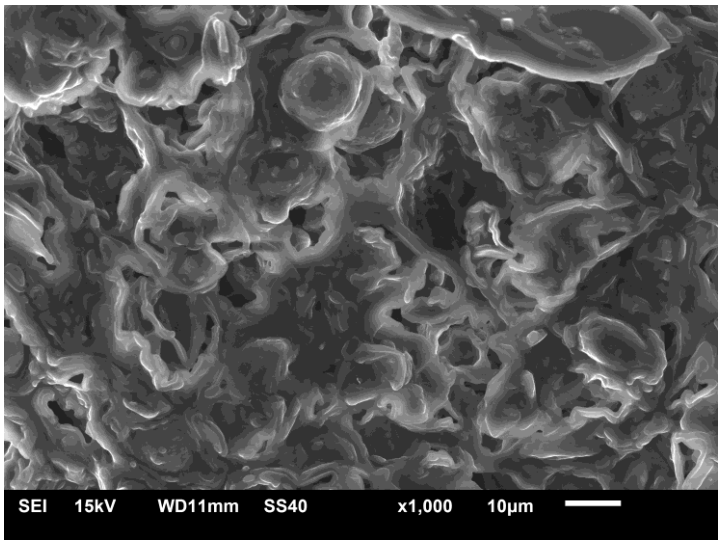

(b)

Figure 3 SEM images of PGS biosorbent.

The SEM images of PGS biosorbent are presented in Figure 3. It can be seen that PGS is composed by irregular particles with a rough surface (Figure 3(a)). Figure 3(a) also confirms the mean diameter of the particles obtained by sieving (from 80 to 110 μm). Several cavities and protuberances can be also visualized in the PGS surface (Figure 3(b)). These characteristics are favorable to accommodate the large dye molecules on the biosorbent surface.

The EDS spectra of PGS biosorbent before (PGS) and after the biosorption process (PGS loaded BB and PGS loaded AR) are shown in Figure 4. It was found that the main elements on the PGS surface before the biosorption process were C, O, P and Mg. These elements are common for biosorbents. However, after the biosorption

process, the element S appeared. This is an indicative that BB and AR dyes (se Figure 1) were biosorbed on the PGS surface. To confirm the EDS results, PGS samples (before and after biosorption) were analyzed in an elemental analyzer (Vario E1–CHNS). The results showed that PGS before biosorption presented traces of S. However, after biosorption, the S percentage was increased. This also confirms the attachment of the dyes on the PGS surface.

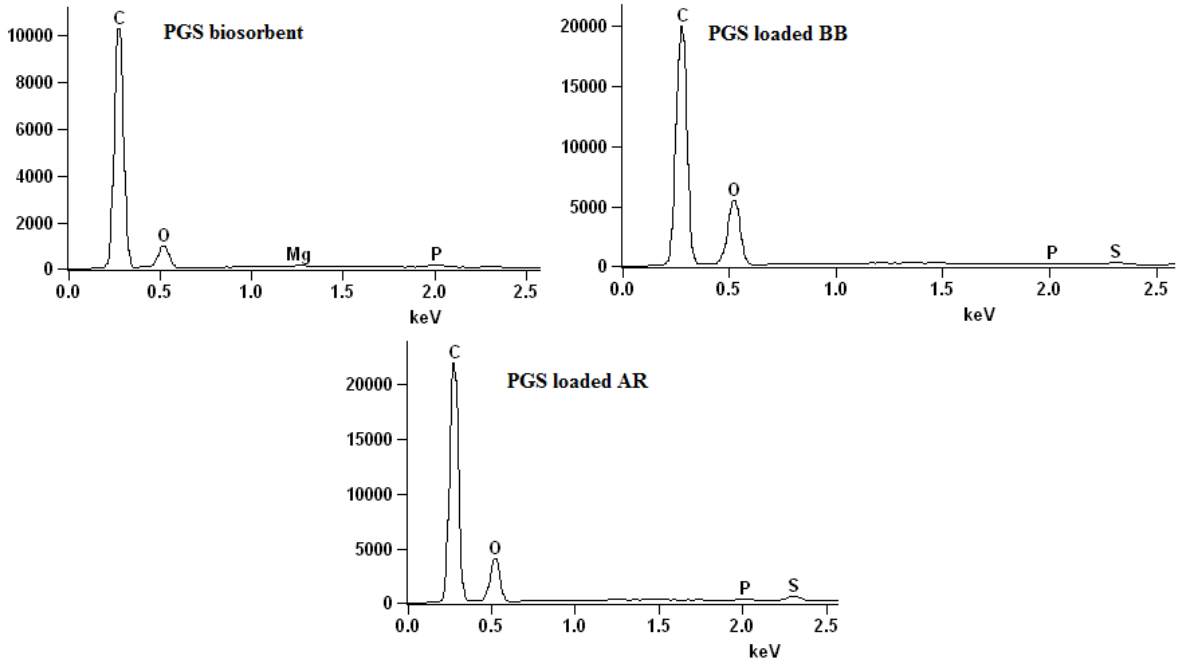

Figure 4 EDS spectra of PGS biosorbent before (PGS) and after the biosorption process (PGS loaded BB and PGS loaded AR).

Effects of initial pH and biosorbent dosage

The effect of initial pH on the biosorption of BB and AR by PGS is presented in Figure 5.

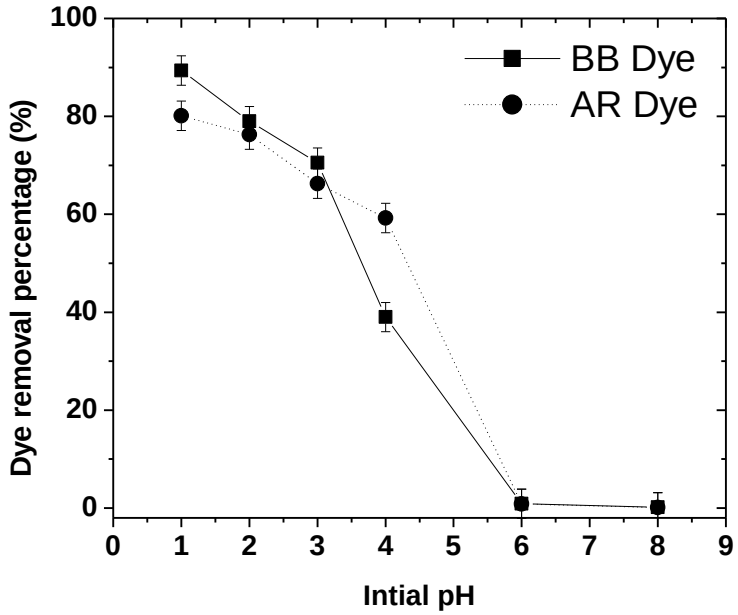

Figure 5 Effect of initial pH on the biosorption of BB and AR dyes by PGS (C_o=50 mg L^{-1}, T=25 °C, t=1 h, V=25 mL, biosorbent dosage=2.00 g L^{-1} and stirring rate=200 rpm).

It can be seen clearly in Figure 5 that the dye removal percentage increased with the pH decrease from 8.0 to 1.0. For both dyes, no biosorption occurred from pH 8.0 to 6.0, while that, the dye removal percentage was higher than 80% at pH 1.0. This shows that the biosorption of BB and AR dyes by PGS is strongly pH dependent. This behavior can be explained on the basis in the characteristics of the PGS and dye molecules. BB and AR are anionic dyes (Figure 1) and its sulphonated groups are negatively charged independent of the pH (since that the pK_a of these groups are negative). In parallel, the PGS biosorbent is positively charged at pH values lower than 6.85 (pH_{zpc} of the biosorbent is 6.85). In this way, at pH of 1.0, the negatively charged dye molecules are attracted by the positively charged surface of the PGS biosorbent, leading to high values of removal percentage. Similar trends were found using other materials to remove BB, like chitosan (Dotto & Pinto 2011), flower wastes (Alvarez & Anaguano 2014) and *Hydrilla verticillata* (Rajeshkannan *et al.* 2011). Also for the removal of AR using chitosan films (Cadaval Jr. *et al*. 2015), water hyacinth leaves (Guerrero–Coronilla *et al*. 2015) and tamarind pod shells (Ahalya *et al*. 2012). Based on these results, the subsequent biosorption tests were performed at pH of 1.0.

The effect of biosorbent dosage on the biosorption of (a) BB and (b) AR dyes by PGS is presented in Figure 6.

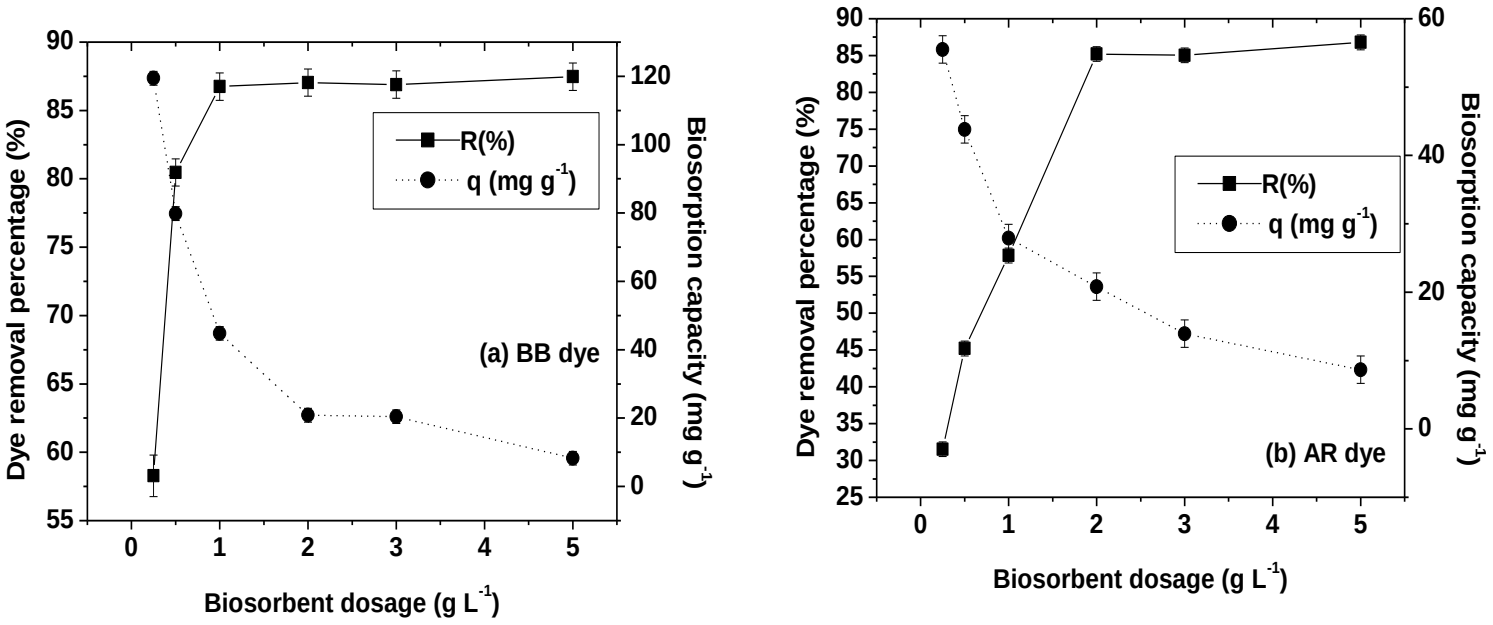

Figure 6 Effect of biosorbent dosage on the biosorption of (a) BB and (b) AR dyes by PGS (C_o=50 mg L^{-1}, T=25 °C, t=1 h, V=25 mL, pH=1.0 and stirring rate=200 rpm).

For BB dye (Figure 6(a)), the increase in biosorbent dosage from 0.25 g L^{-1} to 1.00 g L^{-1} caused an increase from 56 to 87% in the dye removal percentage (R). However, the biosorption capacity (q) decreased from 120 to 40 mg g^{-1}. A new increase from 1.00 g L^{-1} to 5.00 g L^{-1} caused no significant effect on the dye removal percentage but, the biosorption capacity continued to decrease. In the case of AR dye (Figure 6(b)), the increase in biosorbent dosage from 0.25 g L^{-1} to 1.50 g L^{-1} caused an increase from 32 to 85% in the dye removal percentage (R). However, the biosorption capacity (q) decreased from 58 to 18 mg g^{-1}. A new increase from 1.50 g L^{-1} to 5.00 g L^{-1} caused no significant effect on the dye removal percentage but, the biosorption capacity continued to decrease. This behavior is common, since, the increase in biosorbent dosage provides more biosorption sites, and consequently, more dye is removed from the solution. On the other hand, the biosorption capacity decreases, since these additional sites can block one each other. Aiming to obtain suitable values of R and q for both dyes, 0.50 g L^{-1} was selected as the optimum biosorbent dosage to be used in further studies.

Biosorption kinetics

The kinetic curves for the biosorption of BB and AR dyes by PGS were constructed at pH=1.0 with biosorbent dosage of 0.50 g L^{-1}. These curves are depicted in Figure 7.

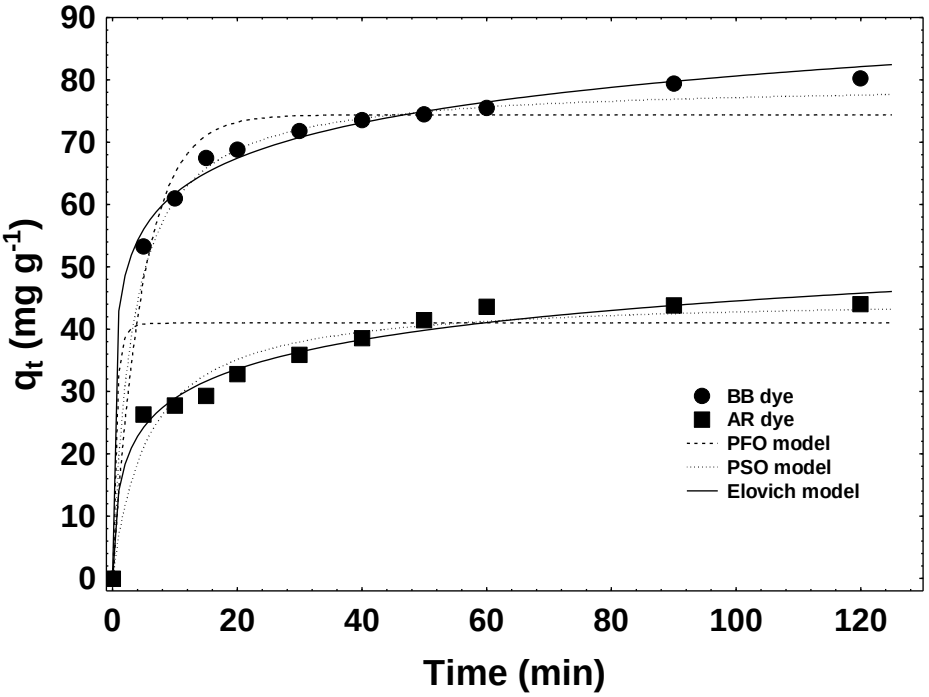

Figure 7 Kinetic curves for the biosorption of BB and AR dyes by PGS (C_o=50 mg L^{-1}, T=25 °C, V=25 mL, pH=1.0, biosorbent dosage=0.50 g L^{-1} and stirring rate=200 rpm).

A typical kinetic behavior was observed for both dyes, where, the biosorption capacity presented a strong increase in the first 5 min, followed by a gradual increase until 90 min. After, the biosorption rate decreased strongly, being that and the equilibrium was attained within 6 h. Also, Figure 6 shows that the biosorption capacity was higher for BB than for AR dye. This can be occurred because that the BB molecule is higher than the AR molecule (see Figure 1), increasing the probability of this molecule be docked in an active site. This behavior was proved in other work, using physical statistics approaches (Dotto *et al.* 2015b).

Pseudo–first order (PFO), pseudo–second order (PSO) and Elovich models were fitted with the experimental data, in order to find an adequate and mathematically easy model to represent the experimental kinetic data. The results are presented in Table 1. The high R^2 and low *ARE* values presented in Table 1 show that the pseudo–second

order (PSO) and Elovich models were adequate to explain the experimental kinetic data. The q_2 value for BB was higher than the q_2 value for AR, confirming its higher biosorption capacity. This behavior is corroborated by the *b* parameter of the Elovich model, which was lower for BB. The k_2 values were similar for both dyes, indicating that the biosorption rate was also similar, during the entire biosorption period. However, the h_0 value was higher for BB, indicating that, at the initial stages, the BB biosorption was faster. Finally, Table 2 show that for both dyes, q_2 closely very well with the experimental value $q_e(exp)$ confirming that the PSO model can be used to predict the experimental values of biosorption capacity.

Table 1 Kinetic parameters for the biosorption of BB and AR dyes on PGS.

Models	Dyes	
	BB	AR
PFO model		
q_1 (mg g^{-1})	74.4	41.0
k_1 (min^{-1})	0.207	0.113
R^2	0.9721	0.9092
ARE (%)	4.37	8.62
PSO model		
q_2 (mg g^{-1})	79.6	45.2
k_2 (g mg^{-1} min^{-1})	0.0040	0.0038
h_0 (mg g^{-1} min^{-1})	25.3	6.15
R^2	0.9959	0.9689
ARE (%)	1.73	5.66
Elovich model		
b (g mg^{-1})	0.122	0.146
a (mg g^{-1} min^{-1})	1533.13	46.69
R^2	0.9959	0.9853
ARE (%)	1.63	3.43
$q_e(exp)$ (mg g^{-1})	80.2	43.9

Biosorption isotherms

Figure 8 present the equilibrium isotherms for the biosorption of (a) BB and (b) AR dyes by PGS. For both dyes a type I isotherm (Thommes *et al.* 2015) was observed, with an initial curved portion at lower concentrations, tending to a plateau at higher concentrations. The plateau was most pronounced for AR dye. This behavior indicates a high affinity between the BB and AR molecules with the PGS surface. Furthermore, it can be seen for both dyes that the biosorption capacity increased with the temperature. This can have occurred because that the temperature increase caused an expansion of the biopolymeric matrix of the biosorbent providing more available biosorption sites. Similar trend was found by Guerrero–Coronilla *et al*. (2015) in the AR adsorption onto water hyacinth leaves, using temperature range from 18 to 50 °C.

In order to find an adequate representation for the equilibrium experimental data, the models named Langmuir, Freundlich and Sips were used. The fitting results are presented in Table 2 (for BB) and Table 3 (for AR). The higher values of R^2 and R^2_{adj} and the lower values of *ARE* (Table 2) indicates that the Langmuir model was the best to represent the biosorption equilibrium for the BB dye. However, for the AR dye, the Sips model was the more adequate.

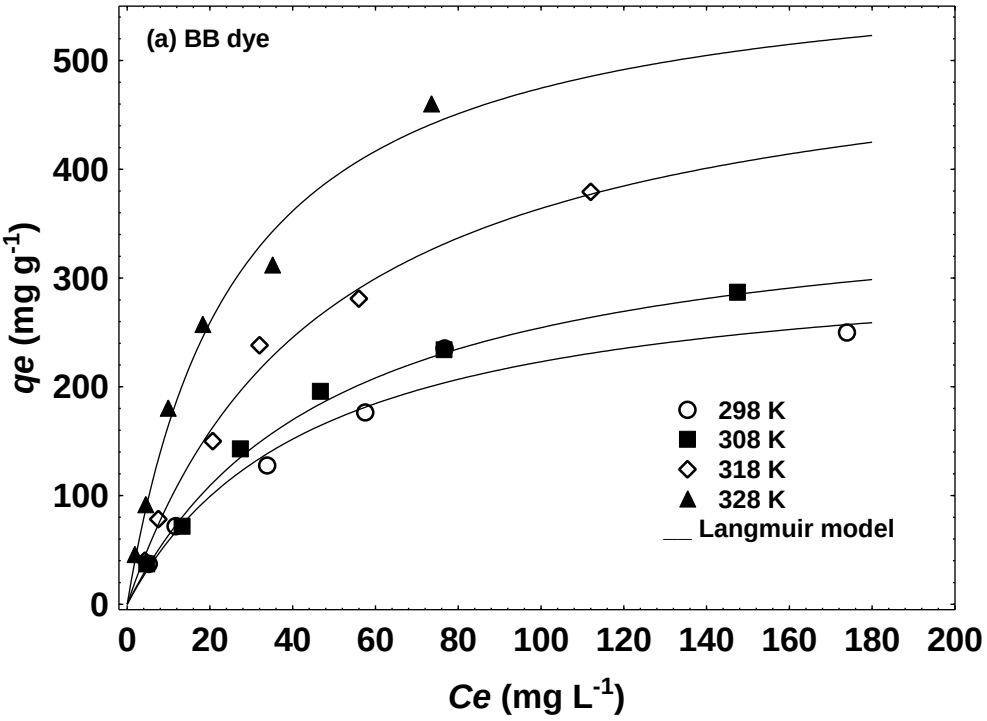

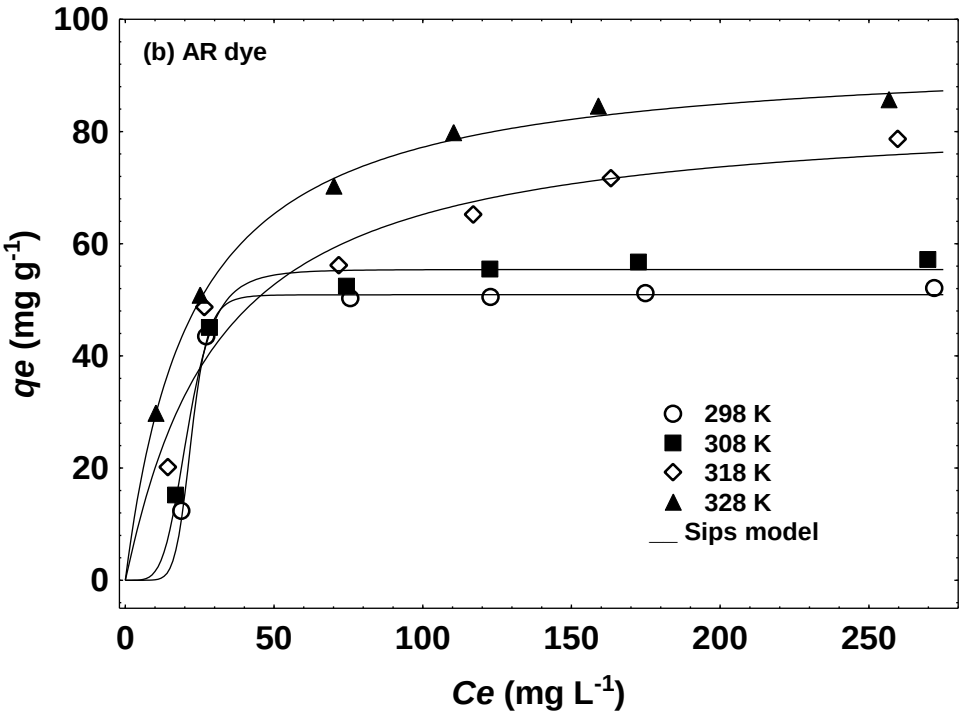

Figure 8 Equilibrium isotherms for the biosorption of (a) BB and (b) AR dyes by PGS (pH=1.0 and biosorbent dosage=0.50 g L^{-1}).

The R_L values of the Langmuir model (Table 2) ranged between 0 and 1, indicating that the BB biosorption was a favorable process. The K_L (Table 2) increased with the temperature, suggesting that the biosorbent–BB affinity was higher at 328 K. The same trend was found for K_s (Table 3). The q_m (BB dye in Table 2) and q_s **(**AR dye in Table 3) parameters increased with the temperature, corroborating that the biosorption capacity is favored at 328 K.

The maximum biosorption capacities were found at 328 K (55 °C) and were 599.5 and 94.2 mg g^{-1} for BB and AR, respectively. A comparison between the maximum biosorption capacities (q_{max}) of several materials used to remove BB and AR dyes from aqueous solutions is presented in Table 4. Based on this table, it can be stated that PGS is an excellent biosorbent to remove BB, since presented a very high biosorption capacity. Also, PGS is a suitable biosorbent for AR, since its biosorption capacity was comparable with the other materials. Furthermore, PGS has low cost, since is obtained from wastes, using a simple processing.

Table 2 Isotherm parameters for BB biosorption onto PGS.

Models	Temperature (K)			
	298	308	318	328
Langmuir				
q_m (mg g^{-1})	324.4	381.6	537.3	599.5
K_L (L mg^{-1})	0.020	0.021	0.022	0.038
R_L (C_0=300 mg L^{-1})	0.131	0.142	0.136	0.080
R^2	0.9790	0.9979	0.9939	0.9985
R^2_{adj}	0.9736	0.9967	0.9918	0.9888
ARE (%)	5.91	4.18	5.76	5.54
Freundlich				
K_F ((mg g^{-1})(mg L^{-1})$^{-1/nF}$)	28.1	26.2	30.1	50.9
$1/n_F$	2.26	2.03	1.83	1.94
R^2	0.9424	0.9717	0.9757	0.9868
R^2_{adj}	0.9303	0.9656	0.9708	0.9834
ARE (%)	16.15	16.15	16.69	13.77
Sips				
q_s (mg g^{-1})	311.8	353.1	515.11	830.1
K_s (L mg^{-1})	0.025	0.024	0.023	0.017
m	1.066	1.111	1.044	0.776
R^2	0.9790	0.9970	0.9930	0.9925
R^2_{adj}	0.9676	0.9950	0.9890	0.9885
ARE (%)	7.42	5.11	5.40	6.96

Table 3 Isotherm parameters for AR biosorption onto PGS.

Models	Temperature (K)			
	298	308	318	328
Langmuir				
q_m (mg g^{-1})	59.8	65.6	85.6	94.4
K_L (L mg^{-1})	0.041	0.040	0.031	0.045
R_L (C_0=300 mg L^{-1})	0.075	0.076	0.097	0.068
R^2	0.8687	0.9218	0.9681	0.9981
R^2_{adj}	0.8415	0.9053	0.9613	0.9972
ARE (%)	22.77	16.04	9.29	1.16
Freundlich				
K_F ((mg g^{-1})(mg L^{-1})$^{-1/nF}$)	14.3	14.7	13.4	20.2
$1/n_F$	4.03	3.84	3.07	3.62
R^2	0.8100	0.8611	0.9493	0.9686
R^2_{adj}	0.7720	0.8332	0.9384	0.9613
ARE (%)	28.59	22.44	12.89	8.32
Sips				
q_s (mg g^{-1})	50.9	55.4	83.9	94.2
K_s (L mg^{-1})	0.045	0.047	0.033	0.048
m	7.994	4.686	1.047	1.006
R^2	0.9999	0.9957	0.9682	0.9989
R^2_{adj}	0.9988	0.9922	0.9522	0.9975
ARE (%)	0.69	1.68	9.24	1.12

Table 4 Comparison between the maximum biosorption capacities (q_{max}) of several materials used to remove BB and AR dyes from aqueous solutions.

Biosorbent	Dye	pH	T (°C)	q_{max} (mg g^{-1})	Reference
PGS	BB	1.0	55	599.5	This work
Chitosan	BB	3.0	25	210.0	Dotto & Pinto (2011)
Flower wastes	BB	2.0	54	40.16	Alvarez & Anaguano (2014)
Hydrilla verticillata	BB	3.0	30	38.46	Rajeshkannan *et al.* (2011)
Mixed sorbents	BB	3.0	30	53.6	Ho & Chiang (2001)

PGS	AR	1.0	55	94.2	This work
Chitosan films	AR	2.0	25	494.13	Cadaval Jr. *et al*. (2015)
Water hyacinth leaves	AR	2.0	18	70.0	Guerrero–Coronilla *et al*. (2015)
Tamarind pod shells	AR	2.0	——	65.04	Ahalya *et al*. (2012)
Alumina reinforced polystyrene	AR	2.0	50	20.23	Ahmad & Kumar (2011)
Activated carbono	AR	1.0	30	166.67	Al–Aoh *et al.* (2013)

Biosorption thermodynamics and interaction mechanism

The biosorption thermodynamic of BB and AR was evaluated according to the standard values of Gibbs free energy change (ΔG^0, kJ mol^{-1}), enthalpy change (ΔH^0, kJ mol^{-1}) and entropy change (ΔS^0, kJ mol^{-1} K^{-1}). The results \are presented in Table 5.

Table 5 Thermodynamic parameters for the biosorption of BB and AR dyes on PGS.

T (K)	BB dye*			AR dye*		
	ΔG^0 (kJ mol^{-1})	ΔH^0 (kJ mol^{-1})	ΔS^0 (kJ mol^{-1} K^{-1})	ΔG^0 (kJ mol^{-1})	ΔH^0 (kJ mol^{-1})	ΔS^0 (kJ mol^{-1} K^{-1})
298	–22.0±0.1	30.2±0.5	0.17±0.02	–19.1±0.1	15.0±0.4	0.11±0.01
308	–22.9±0.1			–20.1±0.1		
318	–24.6±0.2			–20.9±0.1		
328	–27.3±0.2			–22.7±0.3		

* mean±standard error

For both dyes, negative ΔG^0 values were obtained, demonstrating that the BB and AR biosorption onto PGS was a spontaneous and favorable process. The temperature increase provided more negative ΔG^0 values, corroborating that the biosorption was favored at 328 K. The positive ΔH^0 values indicated that the biosorption was endothermic in nature. The endothermic nature was also observed in the malachite green adsorption by Moroccan clay (Elmoubarki *et al.* 2015) (ΔH^0=14.7 kJ mol^{-1}) and reactive blue 19 adsorption on coconut shell activated carbon (Isah *et al.* 2015) (ΔH^0=7.771 kJ mol^{-1}). For both dyes, the magnitude of ΔH^0 values suggests that physical electrostatic interactions occurred. The positive ΔS^0 values indicated some rearrangements on the biosorbent surface during the biosorption.

Based on the FTIR, pH_{zpc}, Boehm titration, pH studies, thermodynamic parameters and dye properties, a possible main biosorption mechanism was proposed: It is know that at pH lower than 6.85 the PGS surface is positively charged. At pH 1.0, the majority of the PGS groups are protonated (basic groups, carboxylic and hydroxyl groups). In parallel, the sulphonated groups of the dye molecules are negatively charged (negative pK_a). Then a physical electrostatic interaction occurs between the dyes and the PGS biosorbent. This mechanism is corroborated by the FTIR spectra, which were not modified after the biosorption and also by the magnitude of ΔH^0 values.

CONCLUSION

In this work, powdered grape seeds (PGS) biosorbent was developed using wastes of a wine industry, and then, applied as an alternative, low cost and efficient material to remove Brilliant Blue (BB) and Amaranth Red (AR) dyes from aqueous solutions. The material characterization revealed that PGS has potential features for biosorption, like functional groups on the surface, cavities and protuberances. The biosorption of BB and AR was favored at pH of 1.0 and biosorbent dosage of 0.50 g L^{-1}, where, the dye removal percentage was higher than 80%. Pseudo–second order and Elovich models were adequate to represent the biosorption kinetic. The biosorption equilibrium of BB on PGS was well represented by the Langmuir model, while for AR, the Sips model was the most adequate. The maximum biosorption capacities were 599.5 and 94.2 mg g^{-1} for BB and AR, respectively, attained at 328 K. The biosorption was a spontaneous, favorable and endothermic process. The biosorption occurred by physical electrostatic interaction between the dyes and the PGS biosorbent. These findings show that PGS is a potential candidate for biosorption purposes, since has low cost, availability, high biosorption capacity and high efficiency.

REFERENCES

Ahalya, N., Chandraprabha, M. N., Kanamadi, R. D. & Ramachandra, T. V. 2012 Adsorption of methylene blue and amaranth on to tamarind pod shells. *Journal of Biochemical Technology* 3 (5), 189–192.

Ahmad, R. & Kumar, R. 2011 Adsorption of Amaranth Dye onto Alumina Reinforced Polystyrene. *Clean – Soil, Air, Water* 39 (1), 74–82.

Ahmed, M. B., Zhou, J. L., Ngo, H. H., Guo, W., Thomaidis, N.S. & Xu J. 2017 Progress in the biological and chemical treatment technologies for emerging contaminant removal from wastewater: A critical review. *Journal of Hazardous Materials* 323 (A), 274–298.

Al Bsoul, A., Zeatoun, L., Abdelhay, A. & Chihad, M. Adsorption of copper ions from water by different types of natural seed materials. *Desalination and Water Treatment* 52 (31–33), 5876–5882.

Al–Aoh, H. A., Jamil Maah, M., yahya, & Radzi Bin Abas, M. 2013 A Comparative Investigation on Adsorption Performances of Activated Carbon Prepared from Coconut Husk Fiber and Commercial Activated Carbon for Acid Red 27 Dye. *Asian Journal of Chemistry* 25 (17), 9582–9590.

Al–Hamamre, Z., Saidan, M., Hararah, M., Rawajfeh, K., Alkhasawneh, H. E. & Al–Shannag, M. 2017 Wastes and biomass materials as sustainable–renewable energy resources for Jordan. *Renewable and Sustainable Energy Reviews* 67 (1), 295–314.

Álvarez, M. S., Moscoso, F., Rodríguez, A., Sanromán, M. A. & Deive, F. J. 2013 Novel physico biological treatment for the remediation of textile dyes–containing industrial effluents. *Bioresource Technology* 146 (1), 689–695.

Anastopoulos, I. & Kyzas, G. Z. 2016 Are the thermodynamic parameters correctly estimated in liquid–phase adsorption phenomena?. *Journal of Molecular Liquids* 218 (1), 174–185.

Belhaine, A., Ghezzar, M. R., Abdelmalek, F., Tayebi, K., Ghomari, A. & Addou A. 2016 Removal of methylene blue dye from water by a spent bleaching earth biosorbent. *Water Science and Technology* 74 (11), 2534–2540.

Cadaval Jr., T. R. S., Dotto, G. L. & Pinto, L. A. A. 2015 Equilibrium Isotherms, Thermodynamics, and Kinetic Studies for the Adsorption of Food Azo Dyes onto Chitosan Films. *Chemical Engineering Communications* 202 (10), 1316–1323.

Crini, G. & Badot, P. M. 2008 Application of chitosan, a natural aminopolysaccharide, for dye removal from aqueous solutions by adsorption processes using batch studies: A review of recent literature. *Progress in Polymer Science* 33 (4), 399–447.

Dotto, G. L. & Pinto, L. A. A. 2011 Adsorption of food dyes onto chitosan: Optimization process and kinetic. *Carbohydrate Polymers* 84 (1), 231–238.

Dotto, G. L., Costa, J. A. V. & Pinto, L. A. A. 2013 Kinetic studies on the biosorption of phenol by nanoparticles from Spirulina sp. LEB 18. *Journal of Environmental Chemical Engineering* 1 (4), 1137–1143.

Dotto, G. L., Pinto, L. A. A., Hachicha, M. A. & Knani, S. 2015b New physicochemical interpretations for the adsorption of food dyes on chitosan films using statistical physics treatment. *Food Chemistry* 171 (1), 1–7.

Dotto, G. L., Santos, J. M. N., Tanabe, E. H., Bertuol, D., Foletto, E. L., Lima, E. C. & Pavan, F. A. 2017 Chitosan/polyamide nanofibers prepared by Forcespinning® technology: A new adsorbent to remove anionic dyes from aqueous solutions. *Journal of Cleaner Production* 144 (1), 120–129.

Dotto, G. L., Sharma, S. K. & Pinto, L. A. A. 2015a Biosorption of organic dyes: Research opportunities and challenges, In: Sharma, S. K. (Ed.), Green Chemistry for Dyes Removal from Waste Water: *Research Trends and Applications. John Wiley & Sons, Beverly, USA.*

Dwyer, K., Hosseinian, F. & Rod, M. 2014 The Market Potential of Grape Waste Alternatives. *Journal of Food Research* 3 (2), 91–106.

Echavarria–Alvarez, A. M. & Hormaza–Anaguano, A. 2014 Flower wastes as a low–cost adsorbent for the removal of acid blue 9. *Dyna 81* (185), 132–138.

El–Khaiary, M. I. & Malash, G. F. 2011 Common data analysis errors in batch adsorption studies. *Hydrometallurgy* 105 (3–4), 314–320.

Elmoubarki, R., Mahjoubi, F. Z., Tounsadi, H., Moustadraf, J., Abdennouri, M., Zouhri, A., El–Albani, A. & Barka, N. 2015 Adsorption of textile dyes on raw and decanted Moroccan clays: Kinetics,equilibrium and thermodynamics. *Water Resources and Industry* 9 (1), 16–29.

Fernández, C., Larrechi, M. S. & Callao, M. P. 2010 An analytical overview of processes for removing organic dyes from wastewater effluents. *Trends in Analytical Chemistry* 29 (10), 1202–1211.

Freundlich, H. 1906 Uber die Adsorption in Losungen. *Zeitschrift fur Physikalische Chemie* 57 (A), 358–471.

Goertzen, S. L., Theriault, K., Oickle, A. M., Tarasuk, A. C. & Andreas, H. A. 2010 Standardization of the Boehm titration: Part I–CO2 expulsion and endpoint determination. *Carbon 48* (4), 1252–1261.

Goldstein, J. I., Newbury, D. E., Echil, P., Joy, D. C., Romig Jr., A. D., Lyman, C. E., Fiori, C. & Lifshin, E. 1992 Scanning electron microscopy and X–ray microanalysis. *Plenum Press*, New York, USA.

Guerrero–Coronilla, I., Morales–Barrera, L. & Cristiani–Urbina, E. 2015 Kinetic, isotherm and thermodynamic studies of amaranth dye biosorption from aqueous solution

onto water hyacinth leaves. *Journal of Environmental Management* 152 (1), 99–108.

Gupta, V. K. & Suhas, I. 2009 Application of low–cost adsorbents for dye removal–a review. *Journal of Environmental Management* 90 (8), 2313–2342.

Hamdaoui, O. & Naffrechoux, E. 2007 Modeling of adsorption isotherms of phenol and chlorophenols onto granular activated carbon Part I: Two–parameter models and equations allowing determination of thermodynamic parameters. *Journal of Hazardous Materials* 147 (1–2), 381–394.

He, Q., Wang, H., Zhang, J., Zou, Z., Zhou, J., Yang, K. & Zheng, L. 2016 Lotus seedpod as a low–cost biomass for potential methylene blue adsorption. *Water Science and Technology* 74 (11), 2560–2568.

Hessel, C., Allegre, C., Maisseu, M., Charbit, F. & Moulin, P. 2007 Guidelines and legislation for dye house effluents. *Journal of Environmental Management 83 (2*), 171–180.

Ho, Y. S. & Chiang, C. C. 2001 Sorption Studies of Acid Dye by Mixed Sorbents. *Adsorption* 7 (1), 139–147.

Ho, Y. S. & Mckay, G. 1998 Kinetic models for the sorption of dye from aqueous solution by wood. *Process Safety and Environmental Protection* 76 (B2), 183–191.

Khandare, R. V. & Govindwar, S. P. 2015 Phytoremediation of textile dyes and effluents: Current scenario and future prospects. *Biotechnology Advances* 33 (8), 1697–1714.

Isah, U., Abdulraheem, G., Bala, S., Muhammad, S. & Abdullahi, M. 2015 Kinetics, equilibrium and thermodynamics studies of C.I. Reactive Blue 19 dye adsorption on coconut shell based activated carbon. *International Biodeterioration & Biodegradation* 102 (1), 265–273.

Lagergren, S. 1898 About the theory of so–called adsorption of soluble substances. Kungliga Svenska Vetenskapsakademiens 24 (4), 1–39.

Langmuir, I. 1918 The adsorption of gases on plane surfaces of glass, mica and platinum. *Journal of the American Chemical Society* 40 (9), 1361–1403.

Liu, Y. & Liu, Y. J. 2008 Biosorption isotherms, kinetics and thermodynamics. *Separation and Purification Technology* 61 (3), 229–242.

Meili L., Silva, T. S., Henrique, D. C., Soletti, J. I., Vieira de Carvalho, S. H., Fonseca, E. J. S., Almeida, A. R. F. & Dotto, G. L. 2017 Ouricuri (*Syagrus coronata*) fiber: a novel

biosorbent to remove methylene blue from aqueous solutions. *Water Science and Technology* 75 (1), 106–114.

Park, J. & Regalbuto, J. R. 1995 A Simple, Accurate Determination of Oxide PZC and the Strong Buffering Effect of Oxide Surfaces at Incipient Wetness. *Journal of Colloid and Interface Science* 175 (1), 239–252.

Pérez–Ibarbia, L., Majdanski, T., Schubert, S., Windhab, N. & Schuber, U. 2016 Safety and regulatory review of dyes commonly used as excipients in pharmaceutical and nutraceutical applications. *European Journal of Pharmaceutical Sciences* 93 (1), 264–273.

Rajeshkannan, R., Rajasimman, M. & Rajamohan, N. 2011 Sorption of Acid Blue 9 Using Hydrilla verticillata Biomass–Optimization, Equilibrium, and Kinetics Studies. *Bioremediation Journal* 15 (1), 57–67.

Silverstein, R. M., Webster F. X. & Kiemle D. J. 2007 Spectrometric Identification of Organic Compounds. *John Wiley & Sons*, New York, USA.

Sips, R. 1948 On the structure of a catalyst surface. *Journal of Chemical Physics* 16 (1), 490–495.

Spiridon, I., Darie–Nita, R. N., Hitruc, G. E., Ludwiczak, J., Spiridon, I. A. C. & Niculaua, M. 2016 New opportunities to valorize biomass wastes into green materials. *Journal of Cleaner Production* 133 (1), 235–242.

Thommes, M., Kaneko, K., Neimark, A. V., Olivier, J. P., Rodriguez–Reinoso, F., Rouquerol, J. & Sing, K. S. W. 2015 Physisorption of gases, with special reference to the evaluation of surface area and pore size distribution (IUPAC Technical Report). *Pure Applied Chemistry* 87 (1), 1051–1069.

Torab–Mostaedi, M., Asadollahzadeh, M., Hemmati, A. & Khosravi, A. 2013 Equilibrium, kinetic, and thermodynamic studies for biosorption of cadmium and nickel on grapefruit peel. *Journal of the Taiwan Institute of Chemical Engineers* 44 (2), 295–302.

Weber, C. T., Collazzo, G. C., Mazutti, M. A., Foletto, E. L. & Dotto, G. L. 2014 Removal of hazardous pharmaceutical dyes by adsorption onto papaya seeds. *Water Science and Technology* 70 (1), 102–107.

Yagub, M. T., Sen, T. K., Afroze, S. & Ang, H. M. 2014 Dye and its removal from aqueous solution by adsorption: A review. *Advances in Colloid and Interface Science* 209 (1), 172–184.

Yedro, F. M., García–Serna, J., Cantero, D. A., Sobrón, F. & Cocero, M. J. 2015 Hydrothermal fractionation of grape seeds in subcritical water to produce oil extract, sugars and lignin. *Catalysis Today* 257 (2), 160–168.

Zeldowitsch, J. 1934 Über den mechanismus der katalytischen oxydation von CO an MnO2. *Acta Physicochemical* URSS 1 (3–4), 449–464.

Zhou, X., Liu, H. & Hao, J. 2012 How to Calculate the Thermodynamic Equilibrium Constant using the Langmuir Equation?. *Adsorption Science &Technology* 30 (1), 647–649.

ANEXO 2

4.2 ARTIGO 2: BIOSORPTION OF SILVER FROM AQUEOUS SOLUTIONS USING WINE INDUSTRY WASTES

L. B. ESCUDERO[1,2]; G. VANNI[3]; F. A. DUARTE[4]; T. SEGGER[4]; G. L. DOTTO[3,*].

[1]Consejo Nacional de Investigaciones Científicas y Técnicas (CONICET), Argentina.
[2]Laboratory of Analytical Chemistry for Research and Development (QUIANID), Facultad de Ciencias Exactas y Naturales, Universidad Nacional de Cuyo, Padre J. Contreras 1300, (5500) Mendoza, Argentina.
[3]Chemical Engineering Department, Federal University of Santa Maria – UFSM, 1000 Roraima Avenue, 97105–900 Santa Maria, RS, Brazil.
[4]Department of Chemistry, Federal University of Santa Maria, UFSM, Santa Maria, RS, Brazil.

Leticia B. Escudero (E–mail address: letibelescudero@gmail.com); Gabriel Vanni (E–mail address: gabrielvnni@gmail.com); Fábio A. Duarte (E–mail address: fabioand@gmail.com); Tássia Segger (E–mail address: tassiaseeger@gmail.com). Guilherme L. Dotto* (E–mail address: guilherme_dotto@yahoo.com.br)

[*]**Corresponding author:** UFSM, 1000 Roraima Avenue, 97105–900, Santa Maria, RS, Brazil. Tel: +55 55 3220 8448; Fax: +55 55 3220 8448. E–mail address: guilherme_dotto@yahoo.com.br

Abstract

The potential of wine industry wastes (grape peel, seed and stem) as alternative biosorbents to remove Ag from aqueous media was investigated in this work. Wine industry wastes were washed, lyophilized and pulverized to obtain the biosorbents. The powdered biosorbents were characterized in detail and several batch experiments were performed to found the most suitable conditions for Ag biosorption. Kinetic, equilibrium, and thermodynamic studies were also carried out. The interactions Ag–biosorbent were elucidated by analyses before and after the biosorption. For all wastes, the maximum removal percentages were found using a biosorbent dosage of 3.0 g L^{-1} at pH of 7.0. The kinetic data were well represented by the pseudo–first order model. The equilibrium was satisfactorily represented by the Sips model. The maximum biosorption capacities, found at 298 K, were: 41.7, 61.4, and 46.4 mg g^{-1} for grape peel, seed, and stem, respectively. Thermodynamically, the biosorption was a spontaneous, favorable, exothermic, and enthalpy–controlled process. The magnitude of ΔH^0 indicated a physical sorption. These results showed that the wine industry wastes can be considered alternative efficient, low–cost, and eco–friendly biosorbents to remove Ag from aqueous media.

Keywords Biosorption; eco–friendly biosorbent; grape; silver; wine wastes.

Nomenclature and units

1/n	Heterogeneity factor, dimensionless
%R	Ag removal percentage, %
a	Desorption constant of the Elovich model, g mg^{-1}.
ARE	Average relative error, %.
b	Initial velocity due to dq/dt with q_t=0, mg g^{-1} min^{-1}.
C_0	Initial Ag concentration in liquid phase, mg L^{-1}.
C_t	Ag concentration in liquid phase at any time, mg L^{-1}.
C_e	Equilibrium Ag concentration in liquid phase, mg L^{-1}.
EDS	Energy X–ray dispersive spectroscopy.
FTIR	Fourier transform infrared spectroscopy.
GPE	Grape peel.
GSE	Grape seeds.
GST	Grape stem.
k_1	Pseudo–first order kinetic constant, min^{-1}.
k_2	Pseudo–second order kinetic constant, g mg^{-1} min^{-1}.
K_D	Equilibrium constant, L g^{-1}.
k_F	Freundlich constant, (mg g^{-1})(mg L^{-1}) $^{-1/n}$.
k_L	Langmuir constant, L mg^{-1}.
k_S	Sips constant, L mg^{-1}.
m	Mass of biosorbent, g.
m_S	Sips exponent, dimensionless.
PFO	Pseudo–first order.
PSO	Pseudo–second order.
pH_{ZPC}	Point of zero charge.
q_1	Biosorption capacity from the pseudo–first order model, mg g^{-1}.
q_2	Biosorption capacity from the pseudo–second order model, mg g^{-1}.
q_t	Mass of Ag biosorbed per gram of biosorbent at any time, mg g^{-1}.
q_e	Mass of Ag biosorbed at equilibrium, mg g^{-1}.
q_m	Maximum biosorption capacity from Langmuir model, mg g^{-1}.
q_S	Maximum biosorption capacity from Sips model, mg g^{-1}.
R	Universal gas constant, J mol^{-1} K^{-1}.

R^2	Coefficient of determination, dimensionless.
R^2_{adj}	Adjusted determination coefficient, dimensionless.
SEM	Scanning electron microscopy.
SSE	Sum of squared error, $mg^2\ g^{-2}$.
t	Time, min.
T	Temperature, K
V	Volume of solution, L.

Greek Symbols

ΔG^0	Standard Gibbs free energy change, kJ mol^{-1}.
ΔH^0	Standard enthalpy change, kJ mol^{-1}.
ΔS^0	Standard entropy change, kJ mol^{-1} K^{-1}.
ρ_w	Solution density, g L^{-1}.

Introduction

Silver (Ag) is a precious metal which has been used in several industries like photographic, electroplating, batteries, and some others (Sari and Tüzen, 2013). As a result of these activities, amounts of Ag are released into the effluents of these industries (Wajima, 2016). It is estimated that around 6% of the Ag present in industrial effluents is directly released into the environment (Muñoz et al., 2017). According to the World Health Organization and the US Environmental Protection Agency, soluble Ag ions are classified as hazardous substances in aqueous media. In addition to the environmental aspects, the economic aspects are also important in this case, since Ag is a precious metal and should be recovered for reuse purposes. In this sense, the removal–recovery of Ag from aqueous media is a first order concern (Tappin et al., 2010; Cantuaria et al., 2016).

Different operations have been used to remove Ag from aqueous media, like separation membrane, chemical precipitation, ion exchange, oxidation, adsorption, and biosorption (Wu et al., 2014; Jeon, 2015; Zhang et al., 2015; Cantuaria et al., 2016). It is clear that each operation has advantages and drawbacks. However, adsorption has gained attention in the last few years, and removal/recovery of Ag has been a very relevant topic (Jeon, 2015). Adsorption is preferred due to some characteristics, including ease of operation, low energetic requirements, and high efficiency (Franco et al., 2017; Dotto et al., 2016a). Activated carbon is the most used adsorbent, but efforts have been performed to test other materials, aiming to make the adsorption operation more attractive and cost–effective. When the adsorbent material is derived from a biomass, adsorption is named biosorption (Dotto et al., 2015). In this sense, the removal of Ag from aqueous media has been studied using macrofungus of *Pleurotus platypus* (Das et al., 2010), activated carbon nanospheres (Song et al., 2011), *Saccharomyces cerevisiae* (Chen et al., 2014), crab shell beads (Jeon, 2015), chitosan gel beads (Zhang et al., 2015), pre–treated bentonite (Cantuaria et al., 2016), and *Klebsiella sp.* 3S1 (Muñoz et al., 2017). The above studies demonstrated the importance of the search and applications of alternative and cheaper materials to remove Ag from aqueous media.

It should be highlighted that, for an effective application of biosorption, the biosorbent should contain the normal characteristics of adsorbents as well as high availability (Dotto et al., 2016b). Wine industry wastes, for example, is an available residue in the Brazil southern and also in Argentina. During the wine production,

around 25% of the grape is discarded as wastes (termed ‘pomace’ which is comprised of skins and seeds) (Dwyer et al., 2014). The management of these wastes is problematic for the industries. Otherwise, pomace contains lignin, cellulose and hemicellulose (Yedro et al., 2015), which can be potential biosorption sites for Ag. In this way, the use of wine industry wastes as alternative biosorbents to remove Ag from aqueous solutions has a synergistic effect, contributing not only for the solid wastes management but also for the treatment of liquid effluents.

This work aimed to verify the applicability of three different wastes from wine industry, including grape peel, grape seeds and grape stem, as alternative biosorbents to remove Ag as Ag(I) from aqueous media. The wastes were obtained from a wine industry located in Mendoza (Argentina), pre–treated, and characterized according to the point of zero charge (pH_{ZPC}), Boehm titration, Fourier transform infrared spectroscopy (FTIR), scanning electron microscopy (SEM), energy X–ray dispersive spectroscopy (EDS), and X–ray mapping. For all wastes, the effects of biosorbent dosage and pH were studied. Biosorption kinetic, equilibrium, and thermodynamic studies were performed. The Ag–biosorbents interactions were also investigated.

Materials and methods

Wine industry wastes: preparation and characterization

The wine industry wastes (peels, seeds, and stems) were collected from a wine industry located in Mendoza province, Argentina. The three materials were manually separated and processed according our previous work (Vanni et al., 2017). In brief, the materials were washed with drinking water and rinsed with Milli–Q water. Then, lyophilization (Virtis freeze mobile, model 6, USA) was performed for 48 h. The dried samples were then pulverized using a mill (Ultracomb, MO–8100A, Argentina) and sieved until the discrete particle size ranging from 80 to 110 μm. The obtained biosorbents were named grape peel (GPE), grape seeds (GSE), and grape stem (GST).

GPE, GSE, and GST biosorbents were characterized according to the point of zero charge (pH_{ZPC}), Boehm titration, Fourier transform infrared spectroscopy (FTIR), scanning electron microscopy (SEM), energy X–ray dispersive spectroscopy (EDS), and X–ray mapping. FTIR, SEM, EDS, and X–ray mapping were performed before and after the biosorption operation, aiming to confirm the biosorption mechanism. The point of zero charge (pH_{ZPC}) was obtained by the eleven points experiment (Park and Regalbuto, 1995). The acidity and basicity was verified by the Boehm titration

(Goertzen et al., 2010). FTIR (Shimadzu, Prestige 21, Japan) was employed to verify the functional groups of the biosorbents (Silverstein et al., 2007). The characteristics and the main elements of the biosorbents surface were assessed by scanning electron microscopy (SEM) coupled to energy X–ray dispersive spectroscopy (EDS) and X–ray mapping (Jeol, JSM–6610LV, Japan) (Goldstein et al., 1992).

Biosorption assays

Batch biosorption experiments were performed in order to verify the effects of initial pH and biosorbent dosage on the biosorption. Initially, pH values between 1–8 (adjusted with 0.1 mol L^{-1} HNO_3/NaOH solutions) were evaluated, using the following conditions: initial Ag concentration of 50 mg L^{-1}, volume of solution of 50 mL, biosorbent dosage of 3.00 g L^{-1}, contact time of 4 h, agitation speed of 200 rpm at a temperature of 298 K, using a thermostated agitator (Marconi, MA 093, Brazil).

The effect of GPE, GSE, and GST dosage (from 0.25 g L^{-1} to 3.00 g L^{-1}) was investigated under the same conditions, using the most adequate pH value defined elsewhere. At the more suitable conditions, kinetic experiments were performed. Thus, 50 ml of 25 and 50 mg L^{-1} of Ag were put in contact with 3 g L^{-1} of each biosorbent and pH was adjusted to 7.0. Then, a contact time of 4 h with an agitation speed of 200 rpm at room temperature was necessary.

The equilibrium experiments were assayed in a thermostatic agitator at 298, 308, 318, and 328 K. Erlenmeyer flasks containing 50 mL of Ag solutions with initial concentrations from 25 to 300 mg L^{-1} were prepared and the pH of each solution was also adjusted to 7.0. The flasks were placed in the thermostatic agitator to reach the suitable temperature. Then, 0.15 g of the biosorbent was added to each flask. The flasks were stirred at 200 rpm until the equilibrium.

After all the experiments, the solid phase was separated by centrifugation (Centribio, 80–2B, Brazil) at 4000 rpm for 20 min and the remaining Ag concentration in the liquid phase was measured by flame atomic absorption spectroscopy (AAS Vario 6, Analytik Jena AG). The experiments were realized in replicate (n=3) using closed vessels and blanks were performed. The Ag removal percentage (%R), mass of Ag biosorbed per gram of biosorbent at any time (q_t (mg g^{-1})) and at equilibrium (q_e (mg g^{-1})) were calculated by the Eqs. (1), (2) and (3), respectively:

$$\%R = \frac{(C_0 - C_t)}{C_0} 100 \quad (1)$$

$$q_t = \frac{V(C_0 - C_t)}{m} \quad (2)$$

$$q_e = \frac{V(C_0 - C_e)}{m} \quad (3)$$

Kinetic models

Information about the biosorption kinetics of Ag onto biosorbents (GPE, GSE, and GST) was found by fitting the following models: pseudo–first order (PFO), pseudo second order (PSO), and Elovich. The kinetic models of PFO and PSO are based on the biosorption capacity (Lagergren, 1898; Ho and McKay, 1998) The PFO model (Eq. (4)) is generally applicable over the initial 20–30 min of sorption process, while the PSO model (Eq. (5)) is suitable for the whole range of contact time.

$$q_t = q_1(1 - \exp(-k_1 t)) \quad (4)$$

$$q_t = \frac{t}{(1/k_2 q_2^2) + (t/q_2)} \quad (5)$$

The Elovich equation (Eq. (6)) is one of the most useful models for describing such activated chemical sorption and is suitable for heterogeneous systems (Liu and Liu, 2008).

$$q_t = \frac{1}{a}\ln(1 + abt) \quad (6)$$

Equilibrium models

The biosorption equilibrium curves of Ag ions on the biosorbents were modeled by the Langmuir (Eq. (7) (Langmuir, 1918), Freundlich (Eq. (8) (Freundlich, 1906), and Sips (Eq. (9) (Sips, 1948) isotherms.

$$q_e = \frac{q_m k_L C_e}{1 + k_L C_e} \quad (7)$$

$$q_e = k_F C_e^{1/n} \quad (8)$$

$$q_e = \frac{q_S (k_S C_e)^{ms}}{1 + (k_S C_e)^{ms}} \quad (9)$$

Thermodynamic parameters

The biosorption thermodynamic parameters like Standard Gibb's free energy change (ΔG^0) (kJ mol^{-1}), standard enthalpy change (ΔH^0) (kJ mol^{-1}) and standard entropy change (ΔS^0) (kJ mol^{-1} K^{-1}) were estimated by the Eqs. (10) and (11) (Milonjic, 2007; Liu, 2009):

$$\Delta G^0 = -RT\ln(\rho_w K_D) \tag{10}$$

$$\ln(\rho_w K_D) = \frac{\Delta S^0}{R} - \frac{\Delta H^0}{RT} \tag{11}$$

where, K_D is the equilibrium constant (L g^{-1}), ρ_w is the solution density (g L^{-1}), T is the temperature (K), and R is the universal gas constant (8.314 J mol^{-1} K^{-1}). The K_D values were estimated from the isotherm model that provided the best fit (Saucier et al., 2015).

Parameters estimation

The parameters of the above models (equilibrium, kinetics, and thermodynamics) were estimated by fitting of the models with the experimental data, using nonlinear regression. The quasi–Newton estimation method was employed and the calculations were performed using Statistica 9.1 software (Statsoft, USA). The determination coefficient (R^2), adjusted determination coefficient (R^2_{adj}), average relative error (ARE), and sum of squared errors (SSE) were used to verify the fit quality (Dotto et al., 2013).

Results and discussion

Characteristics of grape peel, seed and stem biosorbents

All biosorbents were initially characterized according to the point of zero charge (pHzpc). The pHzpc values were 4.30, 6.50, and 4.45 for GPE, GSE, and GST, respectively. This shows that at pH values lower than 4.30, 6.50, and 4.45, the surface of GPE, GSE and GST is positively charged, while it is negatively charged at pH values higher than the pHzpc of each biosorbent. The results of Boehm titrations indicated that all biosorbents were mainly acidic. Table I shows that the amounts of oxygenated groups (carboxylic, lactonic, and phenolic) were 20–30 times higher than the basic groups. This is in accordance with the pHzpc values.

Table 1 Surface chemistry analysis of the biosorbents by Boehm`s titration

Biosorbent	Acidic groups (meq g^{-1})			Basic groups (meq g^{-1})
	Carboxylic	Lactonic	Phenolic	
GPE	0.025 ± 0.001	0.96 ± 0.045	3.16 ± 0.13	0.08 ± 0.004
GSE	0.05 ± 0.003	0.28 ± 0.014	2.98 ± 0.14	0.01 ± 0.0005
GST	0.48 ± 0.016	0.36 ± 0.015	3.40 ± 0.13	0.16 ± 0.0075

The FTIR spectrum is carried out as a qualitative analysis to determine the main functional groups that are involved in the biosorption process (Torab–Mostaedi et al., 2013). Figure 1 shows the FTIR spectra of GPE (a), GSE (b), and GST (c) before and after the biosorption process. From all figures, it is possible verify the major intense bands at 3400 cm^{-1}, which is mainly due to stretching vibration of hydroxyl groups, and at 2900 and 2800 cm^{-1}, which are assigned to C–H and CH_2 stretching vibration of aliphatic groups. In Figure 1(a), it can be also observed bands localized at 1625, 1375, and 1100 cm^{-1}, which can be attributed to alkene group (C=C stretching vibration), C–H stretching vibration of alkane groups, and C–O stretching vibration of alcohol groups, respectively. From GSE (Figure 1(b)), it can be visualized signals at 1750 (C=O stretching vibration), 1650 cm^{-1} (C=O stretching vibration), 1510 cm^{-1} (C=C stretching vibration of aromatic groups), 1400 cm^{-1} (–C–H stretching vibration of alkane groups) and the vibrational bands in the region 1300–1000 cm^{-1} that can be assigned to –CO, C–OC, and carboxylic acids. FTIR spectra of GST in Figure 1(c) shows a band at 1625cm^{-1} (C=O stretching vibration), and at 1060 cm^{-1}, which can be are attributed to C–O stretching vibration. After the biosorption process, slight differences in the spectra can be observed, indicating that no significant chemical modifications occurred during the biosorption. According to these data, we can suggest that no links were formed or broken during the biosorption process, indicating that a physical biosorption occurred.

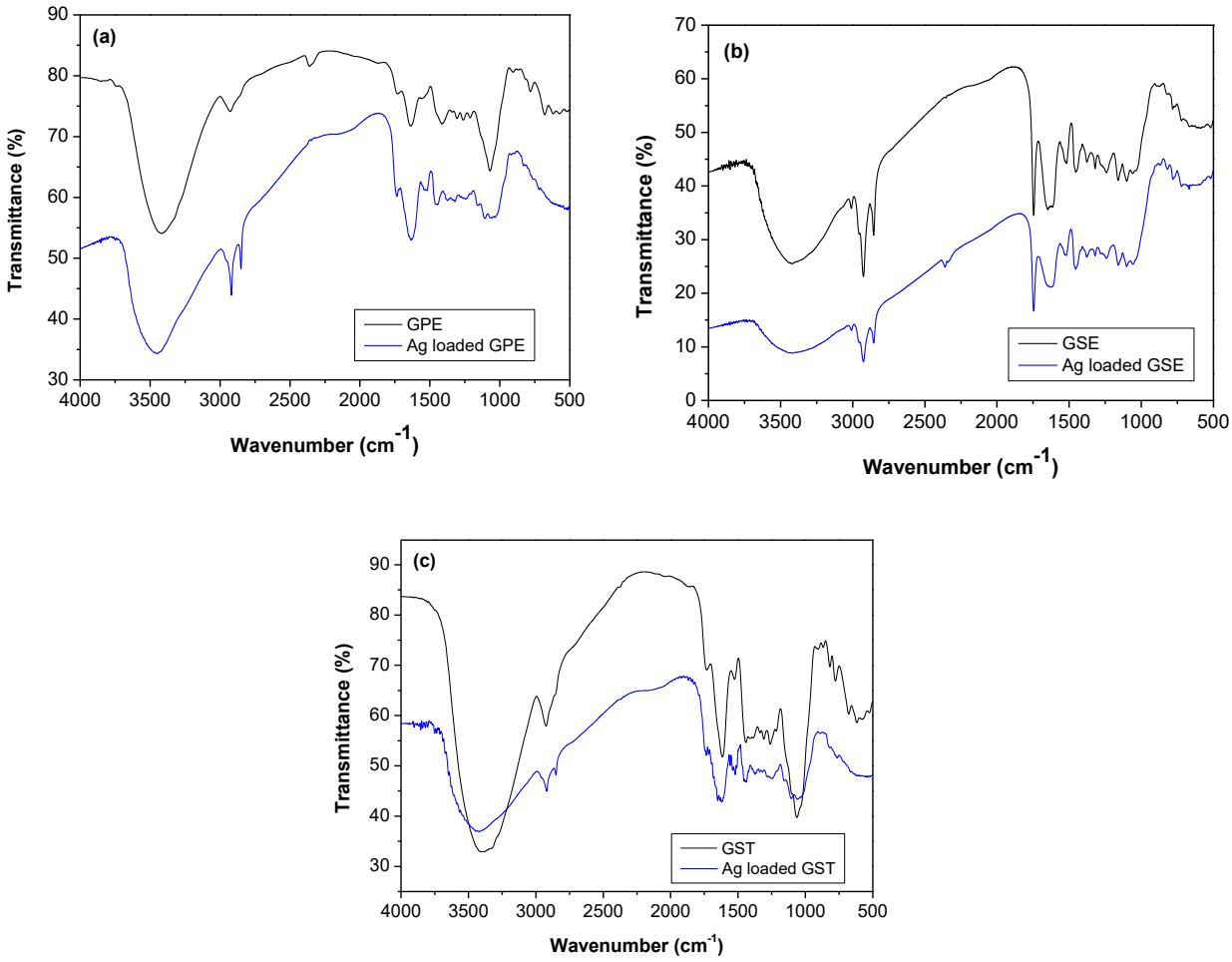

Figure 1: FTIR spectra of GPE and Ag loaded GPE (a), GSE and Ag loaded GSE (b) and GST and Ag loaded GST (c).

Figure 2 shows the energy dispersive X–ray spectra (EDS) of the three biosorbents before and after the biosorption process. Results of the EDS analysis from an average of scanned points showed that the main surface elements of GPE are C, O, and Al (Figure 2(a)). Regarding GSE, the main surface elements are C, O, Mg, P and S (Figure2 (b)). For GST, it can be observed the presence of C, O, and Cl (Figure 2(c)). After biosorption process (Figure 2(d), (e) and (f)), the appearance of Ag can be observed, confirming the effectiveness of Ag ion biosorption onto the oenological wastes.

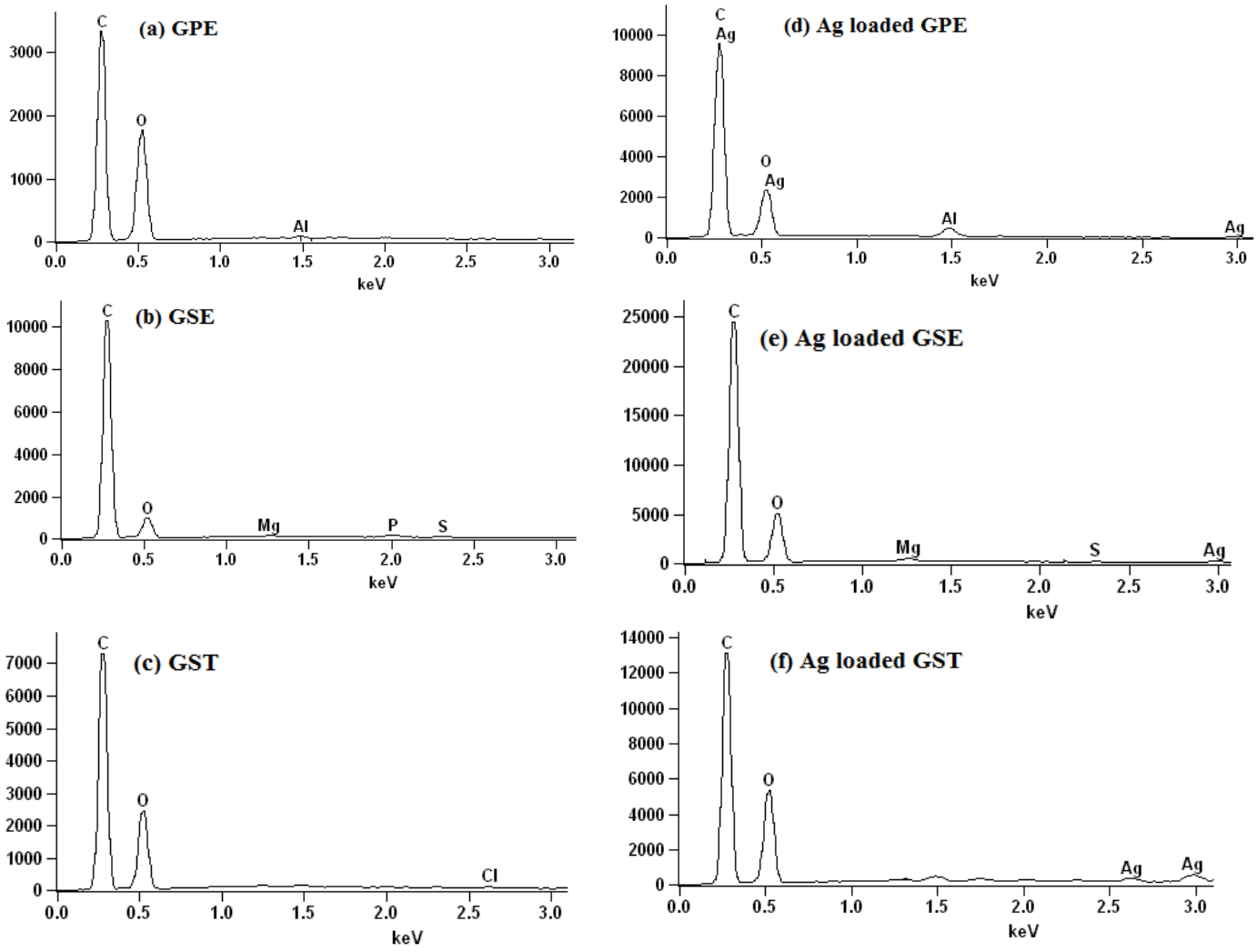

Figure 2: EDS spectra of GPE (a), GSE (b), GST (c), Ag loaded GPE (d), Ag loaded GSE (e) and Ag loaded GST (f).

Scanning electron micrographs were obtained on biosorbents before and after biosorption of Ag ions (Figure 3). Regarding GPE biosorbent, it can be observed a wrinkled and uneven surface before biosorption (Figure 3(a)). After the biosorption process, it could be seen a filling and smoothing surface (Figure 3(d)). This shows that Ag ions covered the external biosorbent surface. On the other hand, the GSE reveals the presence of irregularly placed cavities before biosorption process (Figure3 (b)). After, the biosorbent reveals that the Ag ions had been densely and homogeneously adhered in the surface (Figure 3(e)). The GST biosorbent shows a heterogeneous surface with some cavities and protuberances (Figure 3(c)). After the biosorption, the GST presented the filling of some cavities and apart from that, the surface remained heterogeneous (Figure

3(f)). According to SEM, we can conclude that all the assayed biosorbents obtained good capture of Ag ions on their surfaces.

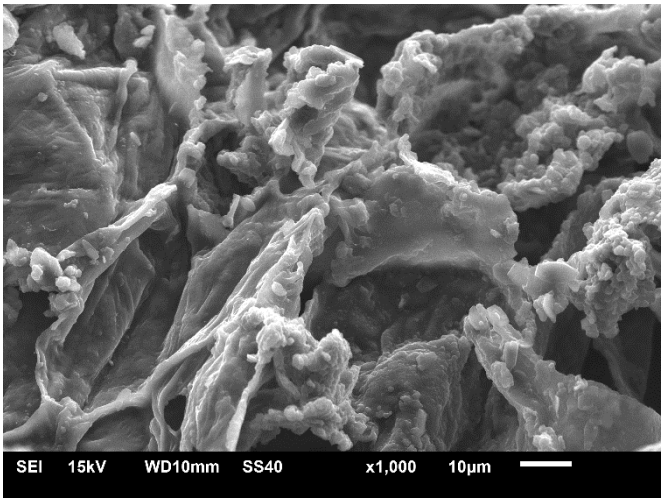

(a)

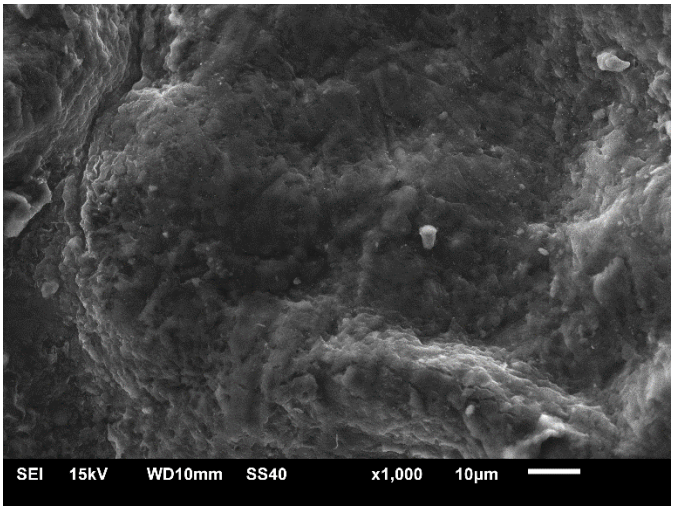

(d)

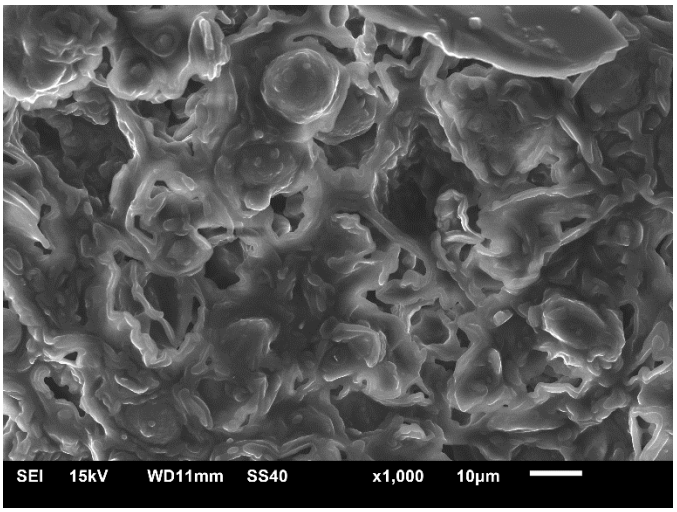

(b)

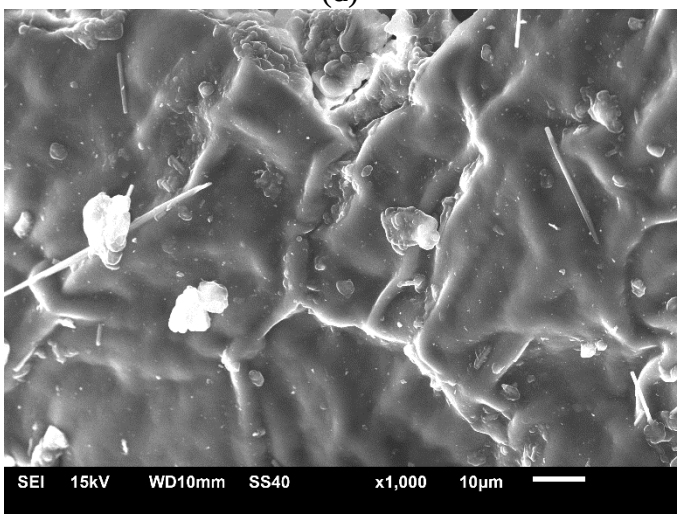

(e)

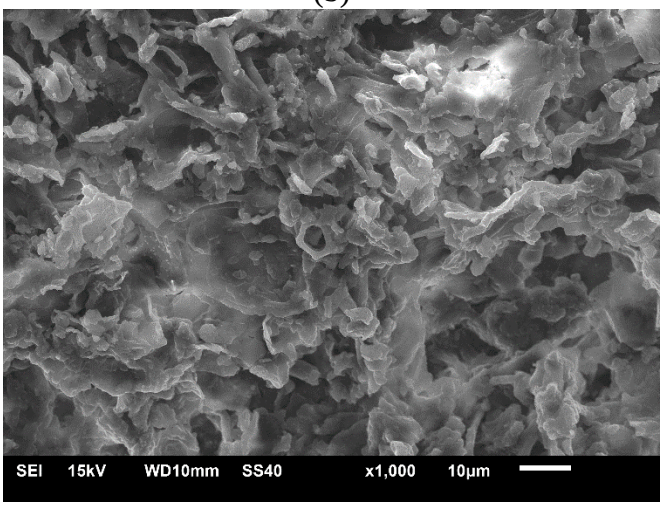

(c)

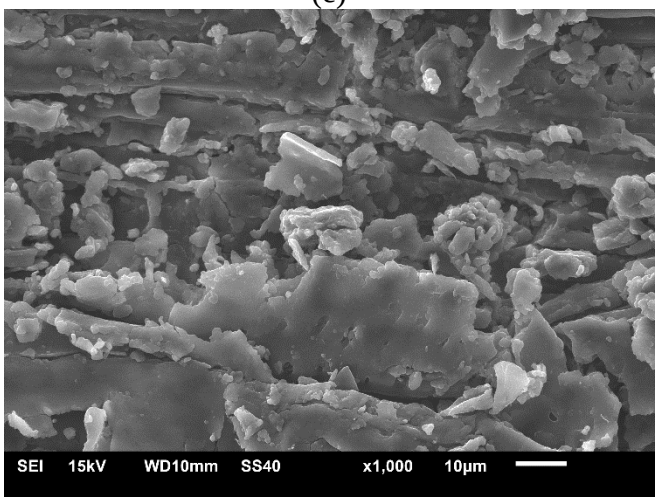

(f)|

Figure 3: SEM images of GPE (a), GSE (b), GST (c), Ag loaded GPE (d), Ag loaded GSE (e) and Ag loaded GST (f).

The X–ray mapping was performed after the biosorption process of Ag ions onto GPE (a), GSE (b) and GST (c) biosorbents (Figure 4). In Figure 4, the violet dots represent Ag ions. It was possible to observe a uniform distribution of Ag ions over the entire surface area of the aforementioned grape–derived materials.

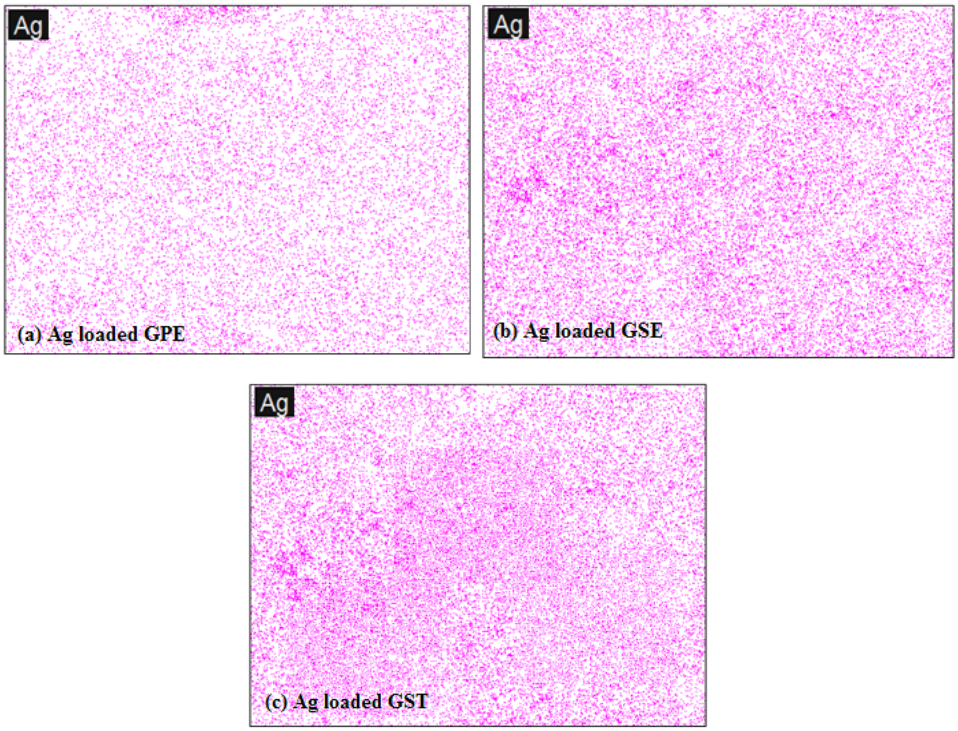

Figure 4: X–ray mappings of Ag loaded GPE (a), Ag loaded GSE (b) and Ag loaded GST (c).

Initial pH and biosorbent dosage effects

The effect of pH on biosorption of Ag ions onto GPE, GSE, and GST is shown in Figure 5 (a), (b), and (c), respectively. Studies beyond pH 8 were not attempted because precipitation of the ions as hydroxides would be likely (Apiratikul and Pavasant, 2006).

Figure 5(a) shows that the Ag ion removal percentage was increased at the pH from 1 to 7, reaching a maximum value at pH 7. At pH 8, it was observed a slight decrease of Ag removal. The maximum Ag ion removal percentage was almost 50%, with a biosorption capacity of GPE higher than 12 mg g^{-1}. For the GSE biosorbent, it could be observed that Ag ion removal percentage increase at the pH from 3 to 6 until it reaches maximum value at pH 7, and a slight decrease of Ag removal was also observed at higher pH values. For this biosorbent, no biosorption occurred from pH 1 and 2 while that, the Ag ion removal percentage was attained almost 50% at pH 7, with a biosorption capacity higher than 13 mg g^{-1}. Regarding GST biosorbent, the Ag ion

removal percentage increases at the pH from 1 to 7, reaching Ag removal higher than 50% at pH 7, with a biosorption capacity of almost 15 mg g^{-1}. According to the pHzpc values previously reported, it can be deduced that at pH of work (pH 7.0), the surface of all biosorbents was negatively charged. In this way, the positive charges of the Ag ions could be attracted by the negatively charged surface of the biosorbents, reaching the high values of metal removal percentage. This behavior can be explained by possible electrostatic interactions between the negative surface of the biosorbents and the positively charge of Ag ions. Similar trend regarding to the pH was found by Wajima (2016), studying the Ag(I) biosorption on a zeolitic material, where the best pH was 6.0. Also at pH 6.0, Jeon (2015) obtained best results for Ag(I) adsorption on immobilized crab shell beads (2.951 mg g^{-1}). In our study, pH 7.0 was selected for the subsequent studies.

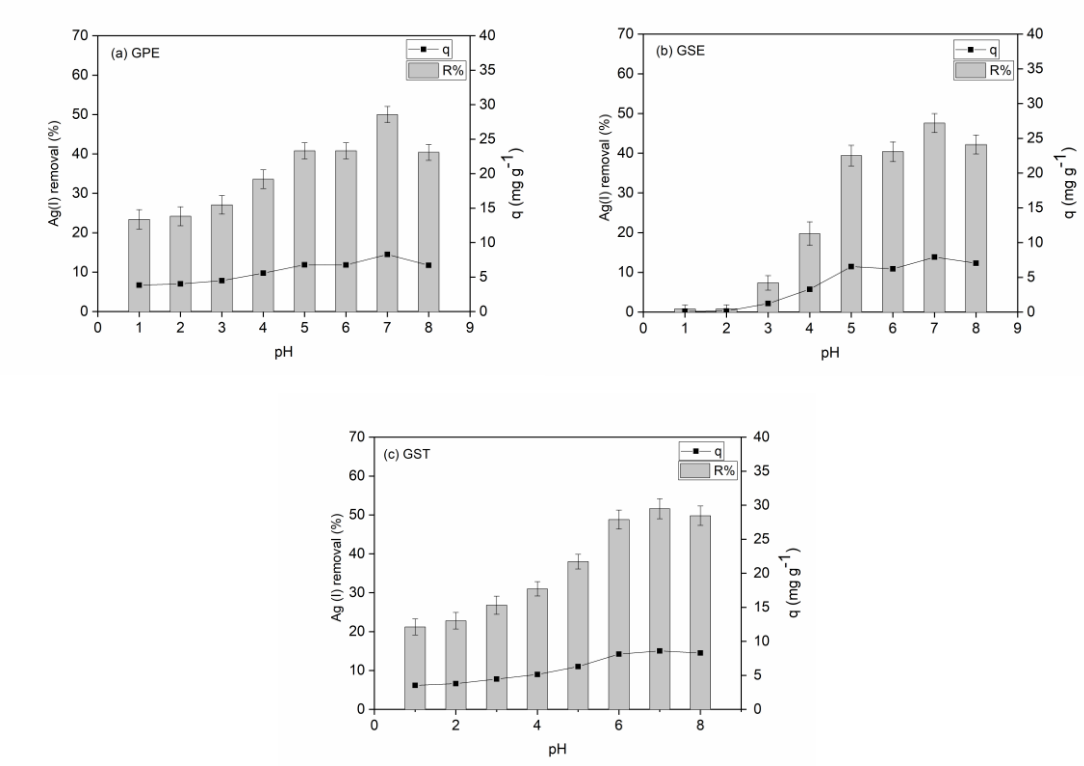

Figure 5: pH effect on the Ag(I) biosorption: GPE (a), GSE (b) and GST (c) (C_0 =50 mg L^{-1}, V = 50 mL, biosorbent dosage of 3.00 g L^{-1}, t = 4 h, 200 rpm, T = 298 K).

The effect of biosorbent dosage is shown in Figure 6. It is possible to note that the increase in biosorbent dosage from 0.25 g L^{-1} to 3.00 g L^{-1} caused an increase in the Ag ion removal percentage (R). However, for the biosorbent (GPE) (Figure 6(a)), the biosorption capacity (q) decreased from 49.4 mg g^{-1} to 12.7 mg g^{-1} when the

biosorption dosage increased from 0.25 g L^{-1} to 1.0 g L^{-1}, after that, the biosorption capacity had a slight decrease from 12.7 mg g^{-1} to 8.4 mg g^{-1} when the biosorbent dosage increased from 1 g L^{-1} to 3 g L^{-1}, where it was reached a maximum value in removal percentage of 51%. For GSE biosorbent (Figure 6(b)), the increase of biosorbent dosage from 0.25 g L^{-1} to 1.5 g L^{-1} caused an increase from 17.3% to 29.7% in the dye removal percentage (R) and the decrease from 29 mg g^{-1} to 9.3 mg g^{-1} in biosorption capacity. Nevertheless, for biosorbent dosage from 1.5 g L^{-1} to 3g L^{-1}, it could be observed an increase in Ag ion removal percentage, reaching a removal of Ag of 49%. For GST biosorbent (Figure 6(c)), it was observed a similar behavior than the previous biosorbents. Taking into account the previous data, the more adequate conditions for all biosorbents were pH 7.0 and biosorbent dosage of 3 g L^{-1}

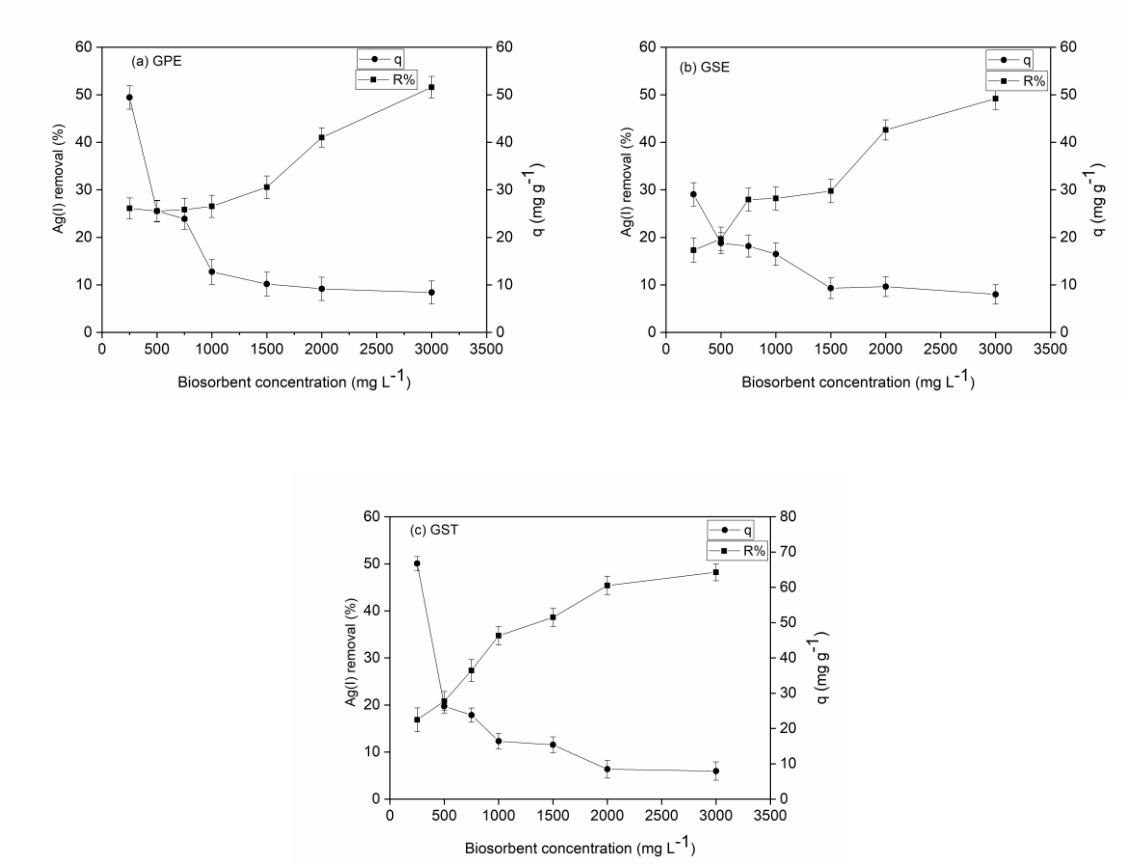

Figure 6: Biosorbent dosage effect on the Ag(I) biosorption: GPE (a), GSE (b) and GST (c) (C_0 =50 mg L^{-1}, V = 50 mL, pH = 7.0, t = 4 h, 200 rpm, T = 298 K).

Biosorption kinetic results

Figure 7 shows the kinetic curves obtained for initial Ag ion concentrations of 25 mg L^{-1} and 50 mg L^{-1} for the three biosorbents. From GPE (Figure 7(a)), it was verified a fast uptake rate in the first stages, reaching biosorption capacities of 7 mg g^{-1} and 2 mg g^{-1}

at 120 min, for initial Ag concentrations of 50 mg L^{-1} and 25 mg L^{-1}, respectively. After this time, the biosorption rate decreased and the biosorption capacity keeps practically constant, reaching maximum values of 8.1 mg g^{-1} and 3 mg g^{-1}. For GSE biosorbent (Figure 7(b)), the curves for the two concentrations followed the same trend until the first 25 min, and then the curve of concentration of 50 mg L^{-1} continued to increase until reaches the equilibrium at 240 min, with a maximum biosorption capacity at 8.2 mg g^{-1}. Regarding GST biosorbent (Figure 7(c)), the trend is similar to the GSE biosorbent during the first 25 min, and then the curves reach almost the maximum biosorption capacities (8.6 mg g^{-1} and 6.9 mg g^{-1} for 50 mg L^{-1} and 25 mg L^{-1} of Ag, respectively).

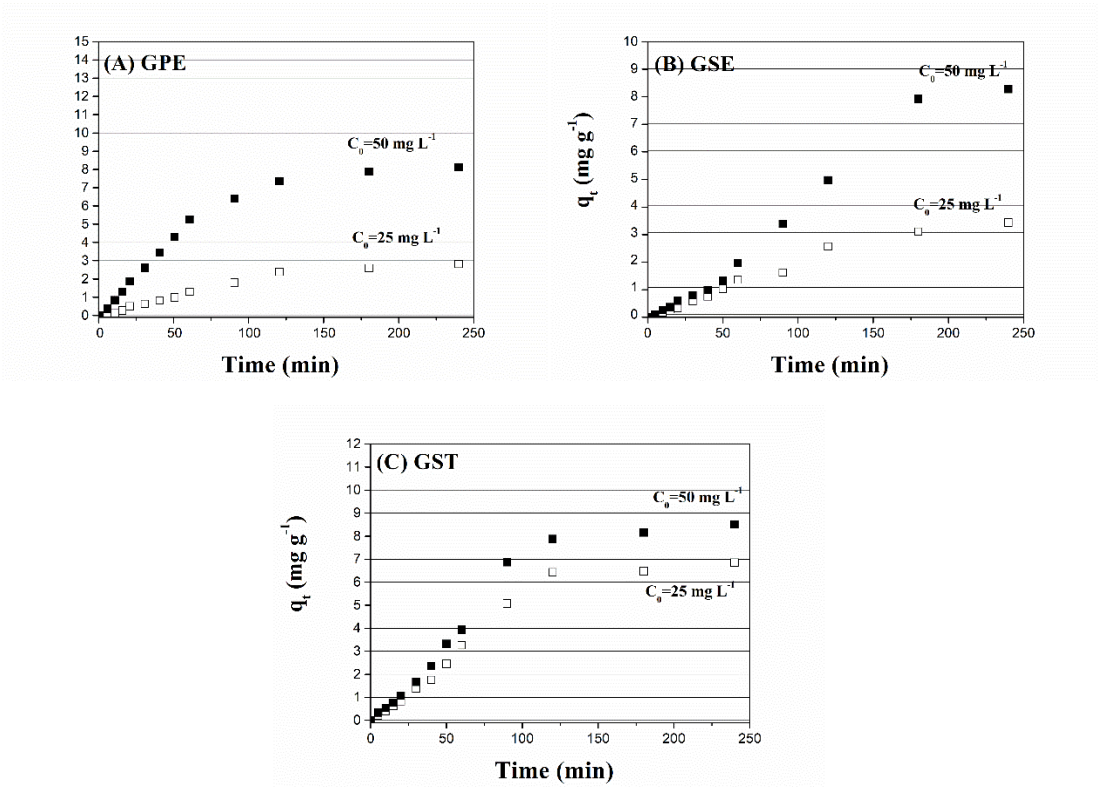

Figure 7: Kinetic curves of the Ag(I) biosorption on GPE (a), GSE (b) and GST (c) (V = 50 mL, pH = 7.0, biosorbent dosage of 3.00 g L^{-1}, 200 rpm, T = 298 K).

The parameters of the kinetic models are given in Table II. Based on the coefficient of determination ($R^2 > 0.95$) and sum of squares errors (SSE < 5.2%), it can be concluded that the pseudo–first order model (PFO) was the most adequate to represent the experimental data and could be used to predict the biosorption kinetic of Ag ions by the wine wastes biosorbents. Comparing the initial concentrations for each

biosorbent, it can be seen that the higher values of q_1 and k_1 were found at 50 mg L^{-1}. For all biosorbents, this confirms that the higher biosorption rate and biosorption capacity were found at 50 mg L^{-1}. Comparing now the biosorbents, it was verified that

Table 2 Kinetic parameters for the Ag(I) biosorption on GPE, GSE, and GST.

Kinetic model	**Grape peel**		**Grape seeds**		**Grape Stem**	
	25 mg L^{-1}	**50 mg L^{-1}**	**25 mg L^{-1}**	**50 mg L^{-1}**	**25 mg L^{-1}**	**50 mg L^{-1}**
Pseudo–first order						
k_1 (min^{-1})	0.007	0.013	0.004	0.005	0.008	0.008
q_1 (mg g^{-1})	3.475	8.704	5.487	12.21	2.952	10.455
R^2	0.992	0.992	0.985	0.966	0.961	0.959
SSE	0.177	0.799	0.235	3.760	0.365	5.112
Pseudo–second order						
k_2 (g mg^{-1} min^{-1})	0.0009	0.0009	0.0004	0.0002	0.001	0.0004
q_2 (mg g^{-1})	5.297	11.856	7.888	16.55	4.566	15.226
h_0 (mg g^{-1} min^{-1})	0.025	0.126	0.003	0.036	0.020	0.092
R^2	0.990	0.984	0.983	0.959	0.955	0.951
SSE	0.223	1.654	0.280	4.574	0.428	6.124
Elovich						
a (g mg^{-1})	0.714	0.383	0.364	0.168	0.825	0.239
b (mg g^{-1} min^{-1})	0.020	0.105	0.017	0.046	0.017	0.067
R^2	0.988	0.973	0.983	0.960	0.949	0.944
SSE	0.270	2.763	0.275	4.444	0.488	6.970
q_{exp} (mg g^{-1})	2.812	8.119	3.433	8.268	6.848	8.501

grape seeds presented the high biosorption capacity, while grape peels presented the high biosorption rate. It is important to highlight that the experimentally determined biosorption capacities (q_{exp}) are similar to those predicted (q_1) by the PFO model.

Biosorption isotherm results

Figure 8 shows the equilibrium isotherms for the biosorption of Ag ion onto (a) GPE, (b) GSE and (c) GST, obtained at 298, 308, 318, and 328 K. Overall, the isotherms of the three biosorbents presented the same favorable behavior, which is characterized by an initial step of increase in biosorption capacity, followed by a convex shape of the curve. All curves can be classified as type "L" normal isotherms. The initial step indicates a great biosorbents–Ag ions affinity and the convex shape suggests the saturation of the biosorption sites by the Ag ions (Giles et al., 1960). Furthermore, it can be seen for the three biosorbents that the biosorption capacity decreased with the temperature increase, indicating an exothermic process. This can be attributed to the fact that at temperatures above 318 K, some damages of sites on the biomasses surface can be occurred and, consequently a decrease in the surface activity is manifested (Aksu, 2005).

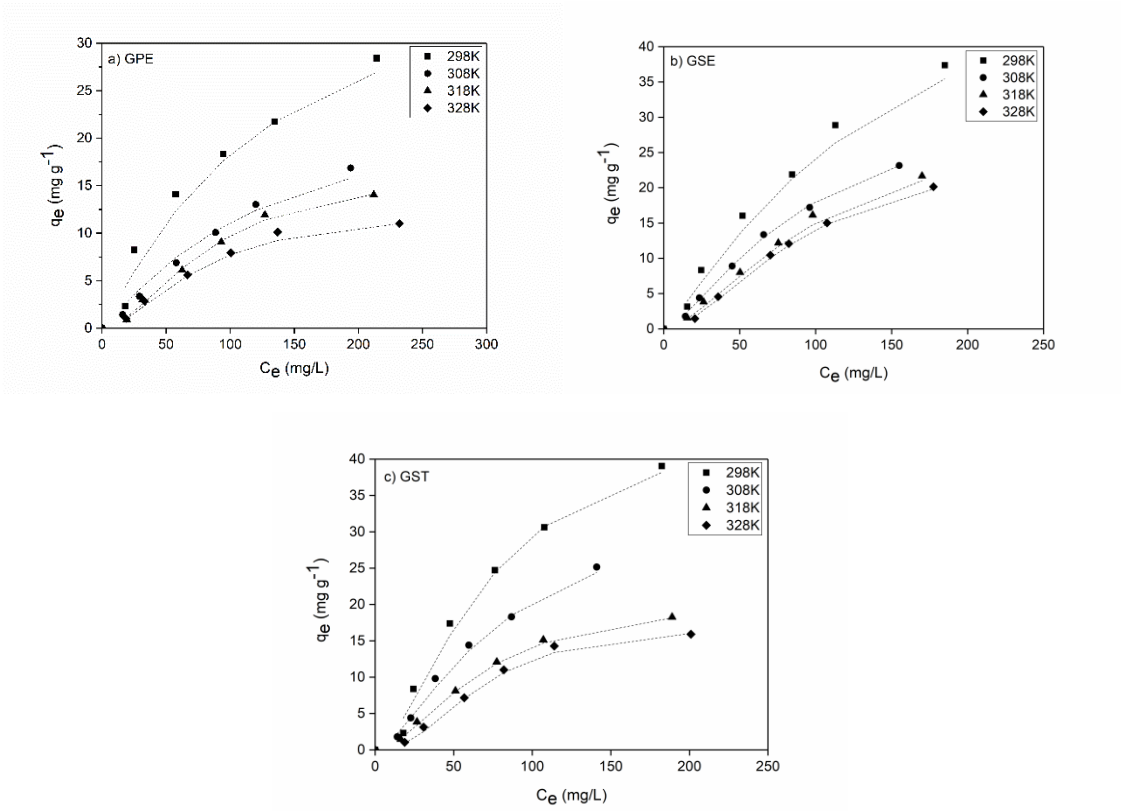

Figure 8: Isotherm curves of the Ag(I) biosorption on GPE (a), GSE (b) and GST (c) (V = 50 mL, pH = 7.0, biosorbent dosage of 3.00 g L^{-1}) (Sips model, ■ 298 K, ● 308 K, ♦ 318 K, ▲ 328 K).

All isotherms were adjusted by Langmuir, Freundlich, and Sips models. The parameters are shown in Table III for all the studied temperaturres.

Table 3 Isotherm parameters for the Ag(I) biosorption on GPE, GSE, and GST.

Isotherm model	Grape peel				Grape seeds				Grape stem			
	298 K	**308 K**	**318 K**	**328 K**	**298 K**	**308 K**	**318 K**	**328 K**	**298 K**	**308 K**	**318 K**	**328 K**
Langmuir												
q_m (mg g^{-1})	48.5	45.8	32.5	20.1	87.0	67.9	71.5	67.7	82.8	76.4	36.9	33.8
k_L (L mg^{-1})	0.006	0.003	0.003	0.005	0.004	0.003	0.002	0.002	0.005	0.003	0.005	0.005
R^2	0.982	0.994	0.976	0.974	0.994	0.992	0.987	0.982	0.978	0.986	0.977	0.951
R^2_{adj}	0.978	0.992	0.971	0.968	0.992	0.990	0.984	0.978	0.973	0.983	0.972	0.941
ARE (%)	20.70	10.059	26.58	19.63	11.49	14.81	17.53	23.34	32.68	21.53	23.03	38.10
SSE	11.17	1.25	4.14	2.96	6.66	3.37	4.74	5.66	27.92	6.85	6.58	11.99
Freundlich												
k_F ((mg g^{-1}) (mg $L^{-1})^{-1/nF}$)	0.938	0.275	0.278	0.367	0.796	0.402	0.307	0.269	0.962	0.442	0.512	0.405
1/n	1.56	1.267	1.34	1.55	1.345	1.232	1.193	1.187	1.384	1.213	0.696	1.405
R^2	0.972	0.986	0.957	0.943	0.985	0.984	0.979	0.973	0.960	0.978	0.953	0.921
R^2_{adj}	0.966	0.983	0.948	0.931	0.982	0.980	0.974	0.967	0.952	0.973	0.943	0.905
ARE (%)	26.43	15.51	32.34	27.80	16.48	18.90	20.79	26.53	40.36	25.55	30.35	44.26
SSE	0.61	3.23	1.26	1.30	15.93	6.87	7.99	8.71	52.10	11.19	13.78	19.40
Sips												
q_S (mg g^{-1})	41.7	25.4	16.8	12.6	61.4	33.8	30.0	25.9	46.4	33.9	21.0	17.3
k_S (L mg^{-1})	0.008	0.008	0.012	0.013	0.007	0.011	0.010	0.011	0.014	0.013	0.015	0.015
ms	1.115	1.138	1.779	1.753	1.206	1.454	1.598	1.770	1.638	1.555	1.787	2.297
R^2	0.983	0.999	0.996	0.995	0.995	0.998	0.998	0.999	0.993	0.996	0.999	0.997
R^2_{adj}	0.974	0.998	0.994	0.992	0.992	0.997	0.997	0.998	0.997	0.994	0.998	0.995
ARE (%)	19.4	2.14	7.46	4.40	8.89	4.60	3.16	4.59	17.57	8.04	3.63	3.81
SSE	10.7	0.08	0.58	0.55	4.64	0.43	0.49	0.22	8.57	1.89	0.20	0.65

A comparison of the R^2, ARE (%), and SSE values was performed for the three models. According to data presented in Table III, it can be observed that the Sips model showed the best adjustment for the three biosorbents. It is important to mention that q_s

parameter decreased with the temperature, corroborating that the biosorption capacity was favored at 298 K. This behavior is attractive from the economic viewpoint, since no requirements of temperature and extra time are required for reaching the maximum biosorption capacity. The maximum biosorption capacities (q_s) reported at 298 K from the Sips model were 41.7 mg g^{-1}, 61.4 mg g^{-1} and 46.4 mg g^{-1} for GPE, GSE, and GST, respectively. Jeon (2015) obtained 2.951 mg g^{-1} for Ag(I) adsorption on immobilized crab shell beads. In the study of Zhang et al. (2015), the maximum uptake of Ag by ion–imprinted chitosan beads was 89.20 mg g^{-1}. Das et al. (2010) obtained biosorption capacity of 46.7 mg g^{-1} using the macrofungus *Pleurotus platypus* as biosorbent. Song et al. (2011) obtained adsorption capacity of 152 mg g^{-1} using surface activated carbon nanospheres as Ag adsorbent. Cantuaria et al. (2016) obtained maximum adsorption capacities of 61.48 mg g^{-1} using Verde–lodo clay for Ag removal. These results indicate that the wine industry wastes (GPE, GSE, and GST) are competitive materials to uptake silver from aqueous media, in terms of biosorption capacity. Other advantages of these biosorbents are low–cost and availability. Furthermore, the use of GPE, GSE, and GST as biosorbents contributes for the solid wastes management in wine industries.

Table 4 Thermodynamic parameters for the Ag(I) biosorption on GPE, GSE, and GST.

T (K)	**ΔG^0 (kJ mol^{-1})**			**ΔH^0 (kJ mol^{-1})**			**ΔS^0 (kJ mol^{-1} K^{-1})**		
	GPE	**GSE**	**GST**	**GPE**	**GSE**	**GST**	**GPE**	**GSE**	**GST**
298	–14.38	–15.00	–16.03	–17.85	–25.48	–28.60	–0.01	0.01	–0.03
308	–13.58	–15.13	–15.56						
318	–13.99	–15.04	–15.17						
328	–13.85	–15.36	–15.11						

Biosorption thermodynamics

Thermodynamic parameters such as ΔG^0, ΔH^0 and ΔS^0 were calculated and are shown in Table IV. For all biosorbents, it was found that the biosorption was a spontaneous and favorable process, since the ΔG^0 values were negative. In general, more negative ΔG^0 values were found at 298 K, indicating that the biosorption was favored in this

temperature. The negative values of ΔH^0 confirm that the Ag biosorption on GPE, GSE, and GST was an exothermic process. The magnitude of ΔH^0 is in agreement with physisorption (Crini and Badot, 2008). Specifically, ΔH^0 values closes with physical electrostatic interactions between the biosorbent and adsorbate, which the magnitude ranges from 20 to 80 kJ mol^{-1} (Bergmann and Machado, 2015). Comparing the values of ΔH^0 with $T\Delta S^0$, it can be seen than ΔH^0 contributes more than $T\Delta S^0$ to reach negative values of ΔG^0. This behavior shows that the Ag biosorption was an enthalpy controlled process.

Interaction mechanism

An interaction mechanism between Ag and the biosorbents was proposed on the basis in the following aspects: FTIR, pHzpc, Boehm titration, Ag speciation, pH effect and thermodynamic results. At pH of 7.0, the biosorbents are negatively charged, since the pHzpc values were 4.30, 6.50, and 4.45 for GPE, GSE, and GST, respectively. In parallel, Ag is monovalent cationic specie in the form of Ag^+. Then, electrostatic interaction between the acidic groups contained in the biosorbents surface and the Ag^+ explains the biosorption. This interaction mechanism is corroborated by the FTIR study, which reveals that no links were formed or broken during the biosorption process, indicating that a physical biosorption occurred. Also, the ΔH^0 values closed with physical electrostatic interactions between the biosorbent and adsorbate.

Conclusion

This work demonstrates the potential of wine industry wastes (grape peel, seed and stem) as biosorbents to remove Ag from aqueous solutions, in order to contribute with the solid wastes management in wine industries. It was found that the wine industry wastes contain acidic character and pHzpc lower than 6.5, being more adequate to uptake cationic species. The more adequate conditions for Ag biosorption were pH 7.0 and biosorbent dosage of 3 g L^{-1}. The biosorption kinetic profile can be represented by the pseudo–first order model. The Sips model was suitable to represent the biosorption isotherms, being the maximum biosorption capacities of 41.7, 61.4, and 46.4 mg g^{-1} for grape peel, seed, and stem, respectively; obtained at 298 K. Biosorption was spontaneous, favorable and exothermic. It is reasonable infer that electrostatic interactions between the negatively charged surface of the wine wastes and Ag^+ was the

main biosorption interaction mechanism. These results show that a possible application for the wine industry wastes, in order to contribute with the solid wastes management in the wine industries, is the Ag(I) uptake from aqueous media.

Acknowledgements

The authors would like to thank National Council for Scientific and Technological Development (CNPq), Consejo Nacional de Investigaciones Científicas y Técnicas (CONICET), Agencia Nacional de Promoción Científica y Tecnológica (FONCYT) (Project PICT−2015−1338), and Universidad Nacional de Cuyo for the financial support.

References

Apiratikul, R., Pavasant, P. (2006). Sorption isotherm model for binary component sorption of copper, cadmium, and lead ions using dried green macroalga *Caulerpa lentillifera*, *Chem. Eng. J.* 119, 135–145.

Aksu, Z. (2005). Application of biosorption for the removal of organic pollutants: a review, *Proc. Biochem.* 40, 997–1026.

Bergmann, C. P., Machado, F. M. (2015). *Carbon Nanomaterials as Adsorbents for Environmental and Biological Applications*, Springer Cham Heidelberg, New York.

Cantuaria, M. L., Almeida Neto, A. F., Nascimento, E. S., Vieira, M. G. A. (2016). Adsorption of silver from aqueous solution onto pre–treated bentonite clay: complete batch system evaluation, *J. Clean. Prod.* 112, 1112–1121.

Chen, C., Wen, D., Wang, J. (2014). Cellular surface characteristics of Saccharomyces cerevisiae before and after Ag(I) biosorption, *Bioresour. Technol.* 156, 380–383.

Crini, G., Badot, P. M. (2008). Application of chitosan, a natural aminopolysaccharide, for dye removal from aqueous solutions by adsorption processes using batch studies: A review of recent literature, *Prog. Polym. Sci.* 33, 399–447.

Das, D., Das, N., Mathew, L. (2010). Kinetics, equilibrium and thermodynamic studies on biosorption of Ag(I) from aqueous solution by macrofungus *Pleurotus platypus*, *J. Hazard. Mater.* 184, 765–774.

Dotto, G. L., Meili, L., Souza Abud, A. K., Tanabe, E. H., Bertuol, D. A., Foletto, E. L. (2016b). Comparison between Brazilian agro–wastes and activated carbon as adsorbents to remove Ni(II) from aqueous solutions, *Water Sci. Technol.* 73, 2713–2721.

Dotto, G. L., Costa, J. A. V., Pinto, L. A. A. (2013). Kinetic studies on the biosorption of phenol by nanoparticles from Spirulina sp. LEB 18, *J. Environ. Chem. Eng.* 1, 1137−1143.

Dotto, G. L., Ocampo–Pérez, R., Moura, J. M., Cadaval Jr., T. R. S., Pinto, L. A. A. (2016b). Adsorption rate of Reactive Black 5 on chitosan based materials: geometry and swelling effects, *Adsorption* 22, 973–983.

Dotto, G. L., Sharma, S. K., Pinto, L. A. A. (2015). *Biosorption of Organic Dyes: Research Opportunities and Challenges*, in: Sharma, S.K. (Ed.), Green Chemistry for Dyes Removal from Waste Water: Research Trends and Applications. Scrivener publishing LLC, Beverly, pp. 295–329.

Dwyer, K., Hosseinian, F., Rod, M. (2014). The Market Potential of Grape Waste Alternatives, *J. Food Res.* 3, 91–106.

Franco, D. S. P., Tanabe, E. H., Dotto, G. L. (2017). Continuous Adsorption of a Cationic Dye on Surface Modified Rice Husk: Statistical Optimization and Dynamic Models, *Chem. Eng. Commun.* 204, 625–634.

Freundlich, H. M. F. (1906). Uber die adsorption in lösungen, *J. Phys. Chem.* 57, 385–470.

Giles, C. H., MacEwan, T. H., Nakhwa, S. N., and Smith, D. (1960). Studies in adsorption part XI: A system of classification of solution adsorption isotherms and its use in diagnosis of adsorption mechanisms and in measurement of specific surface areas of solids, *J. Chem. Soc.* 786, 3973–3993.

Goertzen, S. L., Theriault, K., Oickle, A. M., Tarasuk, A. C., Andreas, H. A. (2010). Standardization of the Boehm titration: Part I–CO2 expulsion and endpoint determination, *Carbon* 48, 1252–1261.

Goldstein, J.I., Newbury, D.E., Echil, P., Joy, D.C., Romig Jr., A.D., Lyman, C.E., Fiori, C., Lifshin, E. (1992). *Scanning electron microscopy and X–ray microanalysis*, Plenum Press, New York.

Ho, Y. S., McKay, G. (1998). A comparison of chemisorption kinetic models applied to pollutant removal on various sorbents, *Proc. Saf. Environ. Prot.* 76, 332–340.

Jeon, C. (2015). Adsorption behavior of silver ions from industrial wastewater onto immobilized crab shell beads, *J. Ind. Eng. Chem.* 32, 195–200.

Lagergren, S. (1898). About the theory of so–called adsorption of soluble substances, *Kung. Sven. Vetenskap. Hand.* 24, 1–39.

Langmuir, I. (1918). The adsorption of gases on plane surfaces of glass, mica and platinum, *J. Am. Chem. Soc.* 40, 1361–1403.

Liu, Y. (2009). Is the Free Energy Change of Adsorption Correctly Calculated?, *J. Chem. Eng. Data* 54, 1981–1985.

Liu, Y., Liu, Y.J. (2008). Biosorption isotherms, kinetics and thermodynamics, *Sep. Purif. Technol.* 61, 229–242.

Milonjic, S. K. (2007). A consideration of the correct calculation of thermodynamic parameters of adsorption, *J. Serbian Chem. Soc.* 72, 1363–1367.

Muñoz, A. J., Espínola, F., Ruiz, E. (2017). Biosorption of Ag(I) from aqueous solutions by *Klebsiella* sp. 3S1, *J. Hazard. Mater.* 329, 166–177.

Park, J., Regalbuto, J. R. (1995). A Simple, Accurate Determination of Oxide PZC and the Strong Buffering Effect of Oxide Surfaces at Incipient Wetness, *J. Colloid Interface Sci.* 175, 239–252.

Sari, A., Tüzen, M. (2013). Adsorption of silver from aqueous solution onto raw vermiculite and manganese oxide–modified vermiculite, *Micro. Meso. Mater.* 170, 155–163.

Saucier, C., Adebayo, M. A., Lima, E. C., Cataluña, R., Thue, P. S., Prola, L. D. T., Puchana−Rosero, M. J., Machado, F. M., Pavan, F. A., Dotto, G. L. (2015). Microwave–assisted activated carbon from cocoa shell as adsorbent for removal of sodium diclofenac and nimesulide from aqueous effluents, *J. Hazard. Mater.* 289, 18−27.

Silverstein, R. M., Webster, F. X., Kiemle, D. J. (2007). *Spectrometric identification of organic compounds*, John Wiley & Sons, New York.

Sips, R. (1948). On the structure of a catalyst surface, *J. Chem. Phys.* 16, 490–495.

Song, X., Gunawan, P., Jiang, R., Leong, S. S. J., Wang, K., Xu, R. (2011). Surface activated carbon nanospheres for fast adsorption of silver ions from aqueous solutions, *J. Hazard. Mater.* 194, 162–168.

Tappin, A. D., Barriada, J. L., Braungardt, C. B., Evans, E. H., Patey, M. D., Achterberg, E. P. (2010). Dissolved silver in European estuarine and coastal waters, *Water. Res.* 44, 4204–4216.

Torab–Mostaedi M., Asadollahzadeh M., Hemmati A., Khosravi A. (2013). Equilibrium, kinetic, and thermodynamic studies for biosorption of cadmium and nickel on grapefruit peel, *J. Taiwan Inst. Chem. Eng.* 44, 294–301.

United States Environmental Protection Agency (EPA) (1991). Guidance manual for compliance with the filtration and disinfection requirements for public water systems using surface water sources, EPA, Washington (1991)

Vanni, G., Escudero, L. B., Dotto, G. L. (2017). Powdered grape seeds (PGS) as an alternative biosorbent to remove pharmaceutical dyes from aqueous solutions, *Water Sci. Technol.* 76, 1177–1187.

Wajima, T. (2016). Synthesis of zeolitic material from green tuff stone cake and its adsorption properties of silver (I) from aqueous solution, *Micro. Meso. Mater.* 233, 154–162.

World Health Organization (WHO) (2003). Background document for development of WHO Guidelines for Drinking–water Quality: Silver in Drinking–water, WHO 2nd Ed., Geneva.

Wu, J. J., Lee, H. W., You, J. H., Kau, Y. C., Liu, S. J. (2014). Adsorption of silver ions on polypyrrole embedded electrospun nanofibrous polyethersulfone membranes, *J. Colloid Interface Sci.* 420, 145–151.

Yedro, F. M., García–Serna, J., Cantero, D. A., Sobrón, F., Cocero, M. J. (2015). Hydrothermal fractionation of grape seeds in subcritical water to produce oil extract, sugars and lignin, *Catalysis Today* 257, 160–168.

Zhang, M., Helleur, R., Zhang, Y. (2015). Ion–imprinted chitosan gel beads for selective adsorption of Ag+ from aqueous solutions, *Carbohydr. Polym.* 130, 206–212.

5 CONCLUSÃO GERAL

Neste trabalho, os biossorventes casca de uva, semente de uva e engaço de uva foram desenvolvidos usando resíduos da indústria de vinho e aplicados como uma alternativa de baixo custo para remover os corantes Azul Brilhante (AB) e Vermelho Amaranto (VA) como também íons de prata de soluções aquosas, a fim de contribuir com a gestão de resíduos sólidos das indústrias de vinho. Verificou–se que os resíduos da indústria do vinho contêm caráter ácido e pHzpc inferior a 6,85, sendo mais adequados para captar espécies catiônicas. A caracterização dos materiais revelou que esses biossorventes possuem grande potencial de biossorção, uma vez que possuem diversos grupos funcionais em suas superfícies, cavidades e protuberâncias.

Nos experimentos com os corantes AB e VA utilizando a semente, a biossorção foi favorecida em temperatura de 328 K e pH 1, uma vez que em pH menor que 6,85 a superfície da semente é carregada positivamente e as moléculas dos corantes são carregadas negativamente, ocorrendo interação física eletrostática. As máximas capacidades de biossorção foram 599.5 e 94.2 mg g^{-1} para os corantes AB e VA, respectivamente, com biossorção espontânea, favorável e endotérmica. Para os experimentos com os três biossorventes e íons Ag, o processo de biossorção foi favorável em temperatura de 298 K e pH 7,0. As máximas capacidades de biossorção foram: 41,7, 61,4 e 46,4 mg g^{-1} para casca, semente e engaço, respectivamente. A biossorção foi espontânea, favorável e exotérmica.

Os resultados demonstraram que os três biossorventes derivados da indústria de vinho possuem ótima aplicação no processo de biossorção de corantes e prata contribuindo para a gestão de resíduos da indústria de vinho, além de serem materiais competitivos aos já existentes no mercado.

Sugestões para trabalhos futuros

- Investigar o processo de biossorção dos corantes Azul Brilhante e Vermelho Amaranto em modo contínuo;
- Investigar o processo de biossorção dos íons de prata em modo contínuo;
- Aplicar os três biosorventes (GPE, GSE e GST) na remoção de contaminantes contidos em soluções de efluentes reais;
- Produzir carvão ativado do resíduo de semente de uva (GPE) para aplicação no processo de biossorção.
- Investigar o processo de biossorção em leito fluidizado com os três biossorventes.

6 REFERÊNCIAS

ABDOLALI, A. et al. Typical lignocellulosic wastes and by–products for biosorption process in water and wastewater treatment: A critical review. **Bioresource Technology**, v. 160, p. 57–66, 2014.

AKSU, Z. Application of biosorption for the removal of organic pollutants: A review. **Process Biochemistry**, v. 40, n. 3–4, p. 997–1026, 2005.

ARSLAN–ALATON, I.; HANDE, B.; SCHMIDT, J. Advanced oxidation of acid and reactive dyes : Effect of Fenton treatment on aerobic , anoxic and anaerobic processes, **Dyes and Pigments**. v. 78, 2008.

BANAT, I. M. et al. MICROBIAL DECOLORIZATION OF TEXTILE–DYE–CONTAINING EFFLUENTS : A REVIEW, **Bioresource Technology** v. 58, n. 1996, p. 217–227, 1997.

CES Technical Report 113 Low cost biosorbents for dye removal. **Langmuir**, p. 1–136, [s.d.].

CHEN, D. et al. Characterization of anion–cationic surfactants modified montmorillonite and its application for the removal of methyl orange. **Chemical Engineering Journal**, v. 171, n. 3, p. 1150–1158, 2011.

CHEN, G. Electrochemical technologies in wastewater treatment, **Separation and Purification Technology** v. 38, n. September 2003, p. 11–41, 2004.

CHOWDHURY, S. et al. Heavy metals in drinking water: Occurrences, implications, and future needs in developing countries. **Science of the Total Environment**, v. 569–570, p. 476–488, 2016.

DABROWSKI, A. Adsorption – from theory to practice. **Advances in Colloid and Interface Science**, v. 93, p. 135–224, 2001.

DAWOOD, S.; SEN, T. K. Review on Dye Removal from Its Aqueous Solution into Alternative Cost Ef– fective and Non–Conventional Adsorbents. **Journal Chemical Process Enginner**, v. 1, n. 1, p. 1–11, 2014.

DOTTO, G. L. et al. Surface modification of chitin using ultrasound–assisted and supercritical CO2 technologies for cobalt adsorption. **Journal of Hazardous Materials**, v. 295, p. 29–36, 2015.

DOTTO, G. L.; COSTA, J. A. V; PINTO, L. A. A. Kinetic studies on the biosorption of phenol by nanoparticles from Spirulina sp. LEB 18. **Journal of Environmental Chemical Engineering**, v. 1, n. 4, p. 1137–1143, 2013.

DOTTO, G. L.; LIMA, E. C.; PINTO, L. A. A. Biosorption of food dyes onto Spirulina platensis nanoparticles: Equilibrium isotherm and thermodynamic analysis. **Bioresource Technology**, v. 103, n. 1, p. 123–130, 2012.

ERBAY, Z.; ICIER, F. Optimization of hot air drying of olive leaves using response surface methodology. **Journal of Food Engineering**, v. 91, n. 4, p. 533–541, 2009.

FARINELLA, N. V.; MATOS, G. D.; ARRUDA, M. A. Z. Grape bagasse as a potential biosorbent of metals in effluent treatments. **Bioresource Technology**, v. 98, n. 10, p. 1940–1946, 2007.

FAROOQ, U. et al. Biosorption of heavy metal ions using wheat based biosorbents – A review of the recent literature. **Bioresource Technology**, v. 101, n. 14, p. 5043–5053, 2010.

FRANKEL, E. N. et al. Commercial Grape Juices Inhibit the in Vitro Oxidation of Human Low–Density Lipoproteins .**Journal Of Agric. Food. Chem**. v. 8561, n. 97, p. 834–838, 1998.

GHOSAL, P. S.; GUPTA, A. K. SC, Determination of thermodynamic parameters from Langmuir isotherm constant–revisited. **Journal of Molecular Liquids**, 2016.

GUPTA, V. K. et al. Adsorptive removal of dyes from aqueous solution onto carbon nanotubes: A review. **Advances in Colloid and Interface Science**, v. 193–194, p. 24–34, 2013.

GUPTA, V. K.; SUHAS. Application of low–cost adsorbents for dye removal – A review. **Journal of Environmental Management**, v. 90, n. 8, p. 2313–2342, 2009.

HAMDAOUI, O.; NAFFRECHOUX, E. Modeling of adsorption isotherms of phenol and chlorophenols onto granular activated carbon Part I . Two–parameter models and equations allowing determination of thermodynamic parameters. **Journal of Hazardous Materials** v. 147, p. 381–394, 2007.

HASS, I. C. S. Resíduo obtido do processamento do suco da uva, p. 1–124, 2015.

HE, J.; CHEN, J. P. A comprehensive review on biosorption of heavy metals by algal biomass: Materials, performances, chemistry, and modeling simulation tools. **Bioresource Technology**, v. 160, p. 67–78, 2014.

HO, Y. S. et al. KINETICS OF POLLUTANT SORPTION BY BIOSORBENTS : REVIEW. **Separation & Purification** n. June 2013, p. 37–41, [s.d.].

HOLANT, Z. R. Biosorption of Heavy Metals. **Biotechnol Prog**. p. 235–250, 1995.

HUNGER, K.; WILEY–VCH, A. **BOOK Industrial Dyes:** [s.l: s.n.]. v. 125

JAYAPRAKASHA, G. K.; SELVI, T.; SAKARIAH, K. K. Antibacterial and antioxidant

activities of grape (Vitis vinifera) seed extracts. **Food Researh International** v. 36, p. 117–122, 2003.

KONO, H. Preparation and characterization of amphoteric cellulose hydrogels as adsorbents for the anionic dyes in aqueous solutions. **Gels**, v. 1, n. 1, p. 94–116, 2015.

LARGITTE, L.; PASQUIER, R. A review of the kinetics adsorption models and their application to the adsorption of lead by an activated carbon. **Chemical Engineering Research and Design**, 2016.

LIU, Y.; LIU, Y. J. Biosorption isotherms, kinetics and thermodynamics. **Separation and Purification Technology**, v. 61, n. 3, p. 229–242, 2008.

MARIA, L.; MELLO, R. DE. Comunicado155 Técnico. **Embrapa** p. 1–6, 2014.

MELLO, L. M. R.; SILVA, G. A. Disponibilidade e Características de Resíduos Provenientes da Agroindústria de Processamento de Uva do Rio Grande do Sul. **Embrapa: Comunicado Técnico 155**, v. Fevereiro, p. 1–6, 2014.

MOHAN, S. V.; RAO, N. C.; KARTHIKEYAN, J. Adsorptive removal of direct azo dye from aqueous phase onto coal based sorbents : a kinetic and mechanistic study. **Journal of Hazardous Materials**. v. 90, p. 189–204, 2002.

NAYAK, A. et al. Journal of Environmental Chemical Engineering Development of a green and sustainable clean up system from grape pomace for heavy metal remediation. **Biochemical Pharmacology**, v. 4, n. 4, p. 4342–4353, 2016.

NGULUBE, T. et al. An update on synthetic dyes adsorption onto clay based minerals: A state–of–art review. **Journal of Environmental Management**, v. 191, p. 35–57, 2017.

OlSSON, M. Wheat straw and peat for fuel pellets — organic compounds from combustion. **Biomass and bioenergy**, v. 30, p. 555–564, 2006.

PAPER, R. Non–conventional low–cost adsorbents for dye removal : A review. v. 97, p. 1061–1085, 2006.

PRASAD, G.; SINGH, V. N. REMOVAL OF CHROME DYE FROM AQUEOUS SOLUTIONS BY MIXED ADSORBENTS. **Wat. Res.** v. 24, n. 1, p. 45–50, 1990.

ROBINSON, T. et al. Remediation of dyes in textile efluent : a critical review on current treatment technologies with a proposed alternative. v. 77, p. 247–255, 2001.

SANTANA, M. T. A. CARACTERIZAÇÃO FÍSICO–QUIMICA, QUÍMICA E SENSORIAL DE FRUTOS E VINHOS DA (Vitis labrusca L.). 2005.

SAYĞILI, H.; GÜZEL, F.; ÖNAL, Y. SC. Conversion of grape industrial processing waste to activated carbon sorbent and its performance in cationic and anionic dyes adsorption. **Journal of Cleaner Production**, 2015.

SRINIVASAN, A.; VIRARAGHAVAN, T. Decolorization of dye wastewaters by biosorbents: A review. **Journal of Environmental Management**, v. 91, n. 10, p. 1915–1929, 2010.

STAWINSKI, W. et al. Simultaneous removal of dyes and metal cations using an acid, acid–base and base modified vermiculite as a sustainable and recyclable adsorbent. **Science of the Total Environment**, v. 576, p. 398–408, 2017.

SUN, Q.; YANG, L. The adsorption of basic dyes from aqueous solution on modified peat – resin particle. **Wat. Res.** v. 37, n. 821, p. 1535–1544, 2003.

TAYLOR, P. et al. Desalination and Water Treatment Adsorption of copper ions from water by different types of natural seed materials. n. November 2014, p. 37–41, 2013.

THE UNITED NATIONS. Water for People Water for Life. **Water**, p. 36, 2003.

VEGLIO, F.; BEOLCHINI, F. Removal of metals by biosorption : a review. v. 44, p. 301–316, 1997.

VIJAYARAGHAVAN, K.; BALASUBRAMANIAN, R. Is biosorption suitable for decontamination of metal–bearing wastewaters? A critical review on the state–of–the–art of biosorption processes and future directions. **Journal of Environmental Management**, v. 160, p. 283–296, 2015.

YAGUB, M. T. et al. Dye and its removal from aqueous solution by adsorption: A review. **Advances in Colloid and Interface Science**, v. 209, p. 172–184, 2014.